NANOSYSTEMS: PHYSICS, CHEMISTRY, MATHEMATICS, 2019, 10 (3), P. 318–349

The use of nanocluster polyoxometalates in the bioactive substance delivery systems

A. A. Ostroushko[1], I. D. Gagarin[1], I. G. Danilova[1,2], I. F. Gette[1,2]

[1]Ural Federal University named after the first President of Russia B. N. Yeltsin, Ekaterinburg, Russia

[2]Institute of Immunology and Physiology of the Ural Branch of the Russian Academy of Sciences, Ekaterinburg, Russia

alexander.ostroushko@urfu.ru

DOI 10.17586/2220-8054-2019-10-3-318-349

Nanoscale systems occupy the most important place among the vehicles intended for targeted drug delivery. Such vehicles are considered in this review. Attention is paid to the nanocluster polyoxometalate-based systems which are promising for transdermal iontophoretic transport. In this relation, and due to the characteristics of the skin as a transport medium, the problems of the transfer processes modeling are considered.

Keywords: nanocluster polyoxometalates, targeted drug delivery systems, transcutaneous iontophoretic transport.

Received: 3 June 2019

1. Introduction

The development of differently structured nanosystems for targeted delivery of bioactive substances and drugs [1–20] is currently receiving much attention. These systems can improve the drug action efficiency and selectivity, reduce side effects and decrease the dose used. This refers, for example, to cytostatics [21–26], to other drugs and substances, including those that work synergistically and are co-transported together [27–33]. It should be noted in general that the number of reviews and original publications that consider certain aspects of formation and use of the nanostructured targeted delivery systems is large globally and is constantly growing. In particular, Springer Publishing have released a series of books that widely address these matters [34–37]. The present review considers the classification of the organizational levels of the means of targeted drug delivery, including the nano-level, of passive and active methods for implementing delivery processes, and raises some issues related to obtaining these means. The peculiarities of the skin as a transport medium for nanoscale objects, the problems of physical chemistry and mathematical modeling of transcutaneous drug transport, including electrophoretic delivery, are considered. The prospects for using the targeted delivery systems are studied for developing such a class of compounds as polyoxometalates (POM), in particular, molybdenum-containing ones, and their physicochemical properties and metabolic impacts are assessed.

2. Organizational levels of targeted drug delivery systems

2.1. Brief historical note, transition to nanosystems

In his review article [38], Allan S. Hoffman has distinguished three “eras” in the development of targeted drug delivery systems, namely the “MACRO”, “MICRO” and “NANO” eras. In the “MACRO era” times, such controlled release systems as patches, ophthalmic systems for antiglaucoma preparations, silicone-based devices containing contraceptive substances, and systems based on swelling polymer gels [38] were created. The “MICRO era” was characterized by the creation of systems with the sustained release of biodegradable microparticles and of the phase-separated depots. The development of the biodegradable suture polymers was underway in the 1960s and 1970s, and in the 1970s this technology was borrowed for targeted drug delivery and refined to make its clinical use possible in the 1980s. The pioneering work of Langer and Folkman, who showed that proteins could be released from non-degradable polymer matrices, has stimulated researchers to think about alternative ways of drug delivery by using biodegradable polymers [39].

The “NANO era” of targeted or site-controlled systems yielded three key technologies. The first concept is the creation of drugs conjugated to polyethylene glycol (PEG) molecules. The second technology is the “active targeting” of an antibody-conjugated drug to cellular receptors [38]. The third is the use of the “enhanced permeation and retention effect”, the essence of which is in the entrapment of nano-sized carriers within a solid tumor due to the leaky vasculature of a rapidly-growing tumor [40]. In this case, a nanoparticle can serve both as the directly acting agent and as a nanocontainer (core), that is, a carrier for an active agent. In both cases, the development of nanopreparations requires the solution of a number of issues, such as their stability in and safety for the body; delivery to pathological structures, penetration into them and effective impact; as well as elimination from the body (utilization). When

nanocontainers are used, such problems as the transferred agent protection from the destructive influence of the body environment, and the active agent release under the specified conditions arise.

2.2. Microencapsulation as a method preceding the nano-level

It follows from the above that there exist several organizational levels in targeted drug delivery in the body, while the delivery systems can be divided into passive with spontaneous processes of transport and release of active substances, and active (controlled) ones. Passive systems, in particular, protect drugs when administered orally, during their passage through the acidic gastric milieu, and ensure their release in the alkaline environment of the intestine. In this case, the dosed or prolonged release of the active component is possible, to which end various membranes or shells from natural and synthetic materials that form capsules are used. Microencapsulation is one of the trends in the organization of targeted effects of drugs on the body. As is stated above, the bioactive substances can be delivered orally, as well as by introduction into the bloodstream transcutaneously and by other methods. The use of all these delivery routes is usually associated with the creation of protective shells on the so-called nominal units of the delivered drugs (a nominal unit is understood as a spatially separated complex structure (formation) that includes biologically active molecules and/or protective polymer layers, the center of which is a POM particle). Polymeric films for micro- and nano-sized units, as well as the sorbed or chemically bound molecule protectors, serve as protective shells. To regulate the transportation of bioactive substances, e.g., transcutaneously, a special environment with the drug nominal units distributed in it is used. Ointment bases can serve as such an environment, for which hydrophobic, including lipophilic, hydrophilic or diphilic materials are chosen. When choosing ointment bases, their compatibility with drugs is necessary; in some cases, the problem of the ointment base component stability arises [41]. The effect of aprotic dipolar solvents, such as dimethyl sulfoxide, which are universal solvents, on the transcutaneous penetration ability and rate for a large number of substances is well known. Podands and cryptands, the so-called phase transfer catalysts, can be used as the drug transporting molecules. Cryptands are macrocyclic complexones (crown polyesters), while podands are their open-chain analogs [42].

In terms of structure, composition and protective shell, the drug delivery systems can be organized in various ways. Liposomal or vesicular capsules, phospholipid-based structures, e.g., lecithin shells, transport units with shells made of block copolymers or dendrimers, polyelectrolyte multilayer shells are considered promising. The simplest unilamellar liposome is a close to spherical, hollow structure formed by a bilayer of phospholipid molecules. The characteristic size varies from tens of nanometers to tens of micrometers. Humanity has encountered liposome-containing materials long before the formal discovery of these formations. For instance, the chicken egg-based colloidal systems, which contain lecithin, may include some spherical vesicles [43]. The direct discovery of liposomes was preceded by numerous studies. In particular, this is the work of T. N. Gobley, who studied the composition of a number of biological samples, such as chicken eggs, fish eggs, brain tissue of animals and humans, etc. and came to the discovery of lecithin [44]. The chemical nature of lecithin was established by A. Strecker [45]. Liposomes as such were discovered in the 1960s. When studying various blood components, in particular, peculiarities of the phospholipid dispersions behavior A. Bangham *et al.* used the results of electron microscopy to discover that the resulting multilayer structures have obvious similarities with cell membranes [43, 46, 47]. Moreover, this group studied the permeability of the obtained membrane structures and demonstrated that liposome membranes are poorly permeable for ions and large molecules, but are permeable for water and low-molecular weight non-electrolytes [43, 48].

Today, several different liposome types are known. In terms of the number of layers, unilamellar, oligolamellar and multilamellar liposomes are distinguished. In addition, there exist the so-called multi-vesicular liposomes that differ from the multilamellar ones by consisting of smaller liposomes enclosed in a common shell instead of a series of concentrically located layers. Unilamellar liposomes (vesicles) are subdivided into small (SUV) and large (LUV) ones, with a characteristic size of 20–100 for the former, and from 100 nm to several micrometers for the latter. A great multitude of techniques for their production have been developed. Most liposome production methods entail the dissolution of cholesterol, lecithin and the useful "cargo" in an organic solvent, drying to obtain a thin film, and its dispersal in an aqueous medium at a certain temperature to obtain a liposomal suspension [49].

The most common methods include the Bangham method, the reversed-phase evaporation method, and the solvent injection method. According to the thin film hydration method (Bangham method) [50, 51], the first stage involves lipid dissolution in an organic solvent, e.g., chloroform, ethanol, methanol, etc. Then, the solvent is evaporated, e.g., in a rotary evaporator, and a thin lipid film deposits on the vessel walls. The resulting film is dispersed in an aqueous medium. The active substance is loaded into liposomes by the addition to the lipid film (for lipophilic substances), or by the dissolving in the aqueous medium (for hydrophilic substances). This method has a relatively low loading efficiency of 5–15% for hydrophilic preparations. According to the reversephase evaporation method, water or an aqueous buffer solution is added to the lipids dissolved in an organic solvent. Then the organic solvent is evaporated at a reduced pressure. This is the way of obtaining large unilamellar and oligolamellar liposomes [52, 53]. The solvent

dispersion method [50] is mainly used for obtaining unilamellar liposomes. A solution of lipids is prepared in an organic solvent (e.g., in ethanol), and then the solution is quickly injected into the aqueous medium through a narrow channel under pressure [54]. The majority of methods for producing liposomes yield a non-uniform size dispersion of particles, while the Bangham method allows only the production of multilamellar vesicles. In order to reduce the size, to obtain more uniform sizes, as well as to obtain unilamellar liposomes, additional processing is used, in particular, ultrasonic dispersion and extrusion through a special membrane in a French press cell [55–58]. Among the advantages of liposomal systems are the possibility of introducing poorly soluble, lipophilic preparations bound with nonpolar tails of phospholipids forming a liposome; an increased penetrating capacity of drugs through cell membranes due to the affinity of phospholipid membranes of liposomes for cell membranes, and an increased drug bioavailability; and the possibility of extending the action of the rapidly metabolized drugs due to their sustained release. The possibilities of using liposomal means of targeted delivery are reflected in publications of various kinds and different years, e.g., in [2, 4, 5, 59–68]. Among the noted disadvantages of liposomes are their active capture by macrophages, which limits the possibility of drug delivery to a number of organs and tissues, and reduces the time of drug circulation in the body; as well as the liposome membrane degradation caused by lipoproteins. By now, techniques have been developed to circumvent some of the disadvantages of liposomes. Such techniques include the application of a layer of polyethylene glycol (PEG) on the liposome surface [69].

2.3. Nanostructured systems

Metallic and metal-containing nanoparticles form a large class of materials that differ in composition, size and production methods. Some of them have already found their application in biomedicine, and many are considered as promising materials. The presence of a metal core in nanocapsules can contribute to the activation of the drug release due to the local exposure to laser radiation absorbed by the said core with the release of heat (photodynamic, laser therapy). In some cases, the factor contributing to the release of the transported drug from the nanocapsules may be the changing pH of the medium into which they find themselves. By their composition, the metal-containing biomedical nanoparticles are usually divided into purely metallic, e.g., gold copper, silver, and nanoparticles with a complex composition, for example, based on oxides of iron, copper, zinc, titanium, tungsten, on cerium and zirconium dioxides, including those containing rare earth metals [70–86], etc.

There exist various methods for producing nanoparticles [78, 80, 87–102] and compositions on their basis. The most common methods for producing nanoparticles include “soft chemistry” methods, including microreactor [98–100] and hydrothermal [92–97] synthesis, and precipitation (sol-gel method) [87–91]. The methods that are also used include the conductor electric explosion when a high-density current pulse [103–115] is passed through it; direct laser ablation or ablation in a liquid medium [116–132]; methods of the Solution Combustion Synthesis group [133–139], etc. Depending on the role played in biomedicine, the composites can contain both non-magnetic and magnetic nanoparticles [140–162]. One of the trends in the biomedical use of nanoparticles for targeted drug delivery is the creation of compositions where nanoparticles can be used both as a core for attaching the active component and identification systems, and as active carriers. Another trend in nanoparticle application is the magnetic, photodynamic hyperthermia [163–167] of tumors. Magnetic nanoparticles are often used in this case, when they accumulate in a tumor and cause local overheating and destruction of the pathological formation under the influence of an external alternating electromagnetic field. Another function performed by nanoparticles in biomedicine is the visualization of normal and pathological processes, of pathological formations, and the use as biochemical and biophysical sensors.

Gold nanoparticles deserve special mention here, as in recent years they have been actively studied from the point of view of their possible use in biomedical applications. In fact, the attempts to use colloidal gold as a medicine can be found already in Arabic, Indian and Chinese sources dating back to the $5^{th} - 4^{th}$ centuries BC. Colloidal gold has not been overlooked in the medieval Europe either. With varying degree of success, attempts had been made to use it for treating a whole range of illnesses, from mental disorders to infectious diseases. In particular, the medical use of *quinta essentia auri* was mentioned already by Paracelsus (Philippus Aureolus Theophrastus Bombast von Hohenheim) [153] One of the medieval literary sources that has survived until today and describes the process of obtaining colloidal gold and its medical application is a book by Dr. Francisci Antonii [168]. An important property of these nanoparticles is the inherent phenomenon of surface plasmon resonance, the essence of which is in the resonant absorption of incident radiation with a photon energy that corresponds to the energy of the surface plasmon. From the practical point of view, important is the essential dependence of this resonant frequency on what is found on the surface of a gold nanoparticle. Therefore, gold nanoparticles with the identifying molecules (e.g., antibodies) associated with their surface can serve as biochemical sensors by changing the frequency of the absorbed radiation depending on the presence of specific agents (e.g., antigens) in the analyzed medium.

Polymeric nanoparticles with the lipid (oily) core represent one of the subclasses of polymeric nanoparticles. They consist of a lipid core surrounded by a polymeric wall. Such particles have an average size of about 200–300 nm

with a narrow monomodal size distribution. The production of nanocapsules requires, in particular, such materials as polyethers and polyacrylates which are used as polymers, as well as triglycerides, polyatomic alcohols and mineral oils which are used as lipid cores [169]. One of the advantages of the oily-core nanocapsules, as compared to matrix systems, is the large drug loading capacity, especially in the case when the lipophilic nucleus is a good solvent for the loaded drug. Other advantages include the reduced effect of the drug explosive release, drug protection from degradation and the reduction of its side effects. Production of such nanocapsules employs a wide range of oils, including vegetable, mineral oils and individual compounds, such as ethyl oleate. In some cases, the oily core is represented by an active ingredient.

The criteria used to select a material for the oily core include the presence or absence of toxicity, the ability to decompose and/or dissolve the polymer, and the drug holding capacity [169]. Both synthetic and natural biodegradable polymers, including dendrimers, serve as the material for the polymeric nanocapsule walls. Among the polymeric materials are hydrophobic polyethers, such as poly(lactide) (PLA), poly(lactide-coglycolide) (PLGA) and poly(ε-caprolactone) (PCL). Polymers have found wide application in targeted drug delivery due to their biocompatibility and ability to decompose to non-toxic products [169–175]. In addition, the associated drug release kinetics can be controlled by changing the polymer molecular weight. The kinetics of polyester decomposition *in vitro* and *in vivo*, as well as their biological action have been amply studied. They demonstrate slow decomposition by a catalyst, which can be a lipase that determines the lowest immunogenicity [169].

The next important aspect of nanocapsules creation is the surface functionalization. The techniques of surface functionalization can be divided into two groups, namely the attachment of a ligand to a nanocapsule during its creation or after it. In the first case, the polymer is chemically bound to the ligand, and this complex material is used as a raw material for nanocapsules production. In the second case, nonfunctionalized nanocapsules are first created, and then a ligand is attached to their polymer walls during a targeted physicochemical or chemical process. An example of the first approach are nanocapsules covalently bound to polyethylene glycol, the polymer walls of which are made of the diblock copolymer [176–183]. An example of the second approach is the introduction of entire antibodies and their fragments into the surface of the finished nanocapsules [169, 184–186].

Inorganic materials based on layered silicates, titanium oxide, zeolites, functionalized fullerenes and carbon nanotubes are also considered as drug transporting nanoparticles. It has already been noted that the development and use of such means of delivery is impossible without solving the problems of the further fate of sufficiently strong chemical carriers and their behavior in the body after performing their basic functions.

The literature describes hybrid supramolecular structures based on nanocluster polyoxometalates (to be discussed in more detail below) and organic molecules, namely polyelectrolytes. A technique of layer-by-layer synthesis of hybrid nanoparticles based on a latex suspension consisting of spherical polystyrene acrylic acid particles with a negative charge is presented in [187]. As polyelectrolytes, polyallylamine hydrochloride and poly(sodium 4-styrene sulfonate) were used, carrying a positive and negative charge, respectively. The layers of polyelectrolytes alternated with layers of $Mo_{72}Fe_{30}^{n-}$, an iron-molybdenum nanocluster with a negative charge. At the last stage, with all the layers formed, the polystyrene acrylic acid-based core was dissolved in tetrahydrofuran. A study of the obtained structures by scanning electron microscopy showed that they have a spherical structure before and after dissolution of the latex core [187]. It is supposed to use such systems as transport units delivered under the influence of a magnetic field, due to the presence of a magnetic polyoxometallate component in them.

2.4. Carbon-based nanostructured systems

Thanks to their unique properties, carbon-based nanostructured materials attract attention from the point of view of their application in such industries as electronics, materials science, etc. Also, attempts are being made to find application for carbon nanomaterials in nanobiology and nanomedicine for diagnosing pathological conditions and targeted drug delivery. The matter is about three-dimensional (3D) carbon nanostructures (nanodiamonds, in particular), about two-dimensional (2D) structures (graphene), about one-dimensional (1D) structures (nanotubes), and also about zero-dimensional (0D) ones, which include fullerenes and their derivatives. Fullerenes (buckyballs) [188–192] are produced by carbon evaporation, e.g., in an electric arc between two graphite electrodes in helium or other inert gases, or by laser ablation, etc. As a rule, regardless of the method, a mixture of several types of fullerenes is obtained, which is contaminated with graphite, unstructured and cluster inclusions of different composition. Therefore, fullerenes require preliminary purification. Fullerenes can be functionalized by a wide range of molecules through external functionalization (molecules association with the fullerene outer surface) and by metals through internal functionalization (association to the inner surface during synthesis), as well as by replacing carbon atoms with heteroatoms. This aspect makes fullerenes promising candidates as means of targeted drug delivery. However, fullerenes are hydrophobic, which limits the possibilities of their direct use in biomedicine [193] It is possible to obtain their aqueous dispersions [194–200] and associates with organic compounds [200–205]. One of the ways of modifying

the surface of fullerenes provides hydroxylated derivatives such as fullerenols [195, 200, 205, 206, 208]. The specific functionalization of their surface is achieved through the use of amphiphilic polymers, amino acids, carboxylic acids, and biologically active preparations that identify molecules [206, 207]. Fullerenes can be coated with biocompatible materials (encapsulation), e.g., with polyvinylpyrrolidone while conjugates including cytostatic preparations and antibodies to the corresponding cell type, can be used for delivering chemotherapeutic drugs to tumor cells. The absorption of such systems by cells can be realized through specific endocytosis. Another possible trend in the use of fullerenes is the creation of bioactive [203, 204, 206, 208] or contrast materials for nuclear magnetic resonance imaging (MRI) through internal functionalization by contrast agents, including Gd^{3+}, Sc^{3+}, Ho^{3+}, Tm^{2+}, Ga^{3+} and Tc^{2+} ions, with isolation of unstable and potentially toxic contrast materials from the internal medium of the body [209–212]. A similar solution for creating contrast materials is proposed in [213] for Keplerates, the non-carbon analogs of fullerenes which form ionic associates with cations of the above-mentioned metals.

Graphene [214–220], a single-layer (one atom thick) 2D nanostructure possesses high mechanical (high rigidity) and electric transport (high charge carrier mobility) properties, which have drawn attention to it as a material for semiconductor electronics, creating batteries and fuel cells The use of graphene for biomedicine is studied [216, 218], including targeted drug delivery in the form of nanographene oxide (NGO). The discovery and creation of methods for producing carbon nanotubes (CNT) [221] is inextricably linked with the creation of fullerenes, since graphite dispersion in an arc yields not only fullerene molecules, but also one-dimensional CNT structures representing one or several rolled graphite layers [221–247]. The characteristic diameter of a CNT is from one to several nm, while the length reaches tens of μm Among the CNT production methods [221–233] are pyrolytic synthesis, electric arc discharge, chemical vapor deposition, and laser ablation. Targeted CNT synthesis employs d-metal-baseds catalysts [226, 227, 239] (copper, iron, nickel, cobalt, etc.). Most often, the distance between CNT layers is 0.34 nm, which coincides with the distance between the layers in crystalline graphite. As a rule, both ends of a CNT have hemispheres the so-called “caps”, which include pentagons in addition to hexagons, thus making them similar to a half of the fullerene molecule [221, 224]. It is possible to open CNT ends by strong oxidizing agents such as nitric and perchloric acids, or ozone, which open access for various substances to the internal cavity for creating transport systems [237–249]. Methods for CNT size “calibration”using ultracentrifugation, dialysis, and “cutting” them to achieve the desired length have been developed. The synthesized CNTs also have foreign inclusions, including amorphous carbon, graphite and fullerenes. To remove impurities from CNT, technologies for their purification have been developed [235, 236]. By analogy with fullerenes, CNT functionalization can be divided into external and internal. In addition, the non-covalent and covalent types of functionalization are distinguished. Functionalization of the first type is, e.g., CNT surface coating with surfactants, polymers, lipids, etc. The second type includes the reactions of cycloaddition and oxidation under the influence of strong acids, which allow the CNT surface functionalization by carboxyl groups.

The biomedical aspect of nanodiamond use can also be considered [250–260]. The nanodispersed diamonds (or nanodiamonds) were obtained for the first time in in the USSR in the 1960s [261], but the widespread interest in the research of this material arose in the 1990s due to several factors. Among them are the appearance of relatively affordable technologies for nanodiamond production, the use of nanodiamonds as quantum dots instead of toxic semiconductor materials, the development of nanoscale magnetic sensors based on nanodiamonds and some others [254, 262]. The methods of nanodiamond production, like those for producing a number of other superhard materials, are based on the shock compression of the source material. As a rule, the blasting of an explosive creates a shock wave, which makes it possible to achieve the pressure required for the nanodiamond crystal formation. Such synthesis conditions are called dynamic. The chamber in which the shock wave is created can be filled with an inert gas or liquid as a coolant hence, dry and wet synthesis methods exist, respectively. Both the explosive itself and graphite can serve as sources of carbon for the synthesis of nanodiamonds. The characteristic size of diamond crystals obtained by the above-described synthesis methods ranges from a few to tens of nm, and the crystals can also exist in the form of aggregates [264, 265] Methods for disaggregating the obtained material are available [266–269]. In addition to dynamic synthesis, the research on the synthesis under static conditions is underway The composition of impurities in the case with the detonation production method includes carbon in the form of graphite and non-combustible impurities (metals and oxides) [254, 261]. The areas of nanodiamonds application are determined by their inherent outstanding qualities, both characteristic of diamonds in general and specific to nanodiamonds. Such properties as exceptional hardness, the Young’s modulus, specific optical properties, biocompatibility, chemical stability, and fluorescence ability make nanodiamonds a promising material for biomedical applications [250–263]. Among the possible areas of biomedical application is the use as a matrix for tissue engineering, creation of implants and, in particular, bioactive substances targeted delivery [250, 251, 253, 255, 259]. The latter is possible due to the ability of many bioactive substances (proteins, antibodies, nucleic acids, drugs) to bind to the surface of nanodiamonds [253–256, 259, 260, 263]. The use of nanodiamonds as a material for tissue engineering is possible due to their ability to bind to the cell surface, and in

this context studies are being conducted on the use of nanodiamonds as a means of cell delivery for cell therapy, in particular, for bone tissue regeneration [258, 270].

2.5. Features of active drug delivery systems

Active methods of drug delivery to biological targets include, among others, the impact of physical factors on the transported nominal units. These factors include, first of all, the magnetic and electric fields, which implies the creation of a means of delivery with relevant physical properties. The creation of units transported under the influence of a magnetic field is associated with the conjugation of bioactive substances and ferromagnetic particles at the nano- and micro levels. Associates may also include the above-mentioned protective shells in this case, too. The use of the magnetic phase-based associates should ensure not only targeted drug delivery to the correct location in the body, but also the subsequent safe removal of solid particles from it. This technique requires the use of magnetic fields of sufficiently high intensity. As is noted above, magnetic particles can be used for magnetic hyperthermia simultaneously with the delivery of drugs.

Electric field-assisted delivery (electrophoresis, iontophoresis) is acceptable for substances that form charged units at the level of ions or colloidal particles. It is well known that a fairly wide range of bioactive substances and drugs can be delivered to the body iontophoretically, including transcutaneous delivery. Such a delivery option significantly increases its efficiency and does not require the application of high intensity electric fields. Actually, the effect of iontophoresis on the skin increases its permeability to bioactive substances. In a number of cases, iontophoresis can be carried out directly for the drugs that form ions and amphiphilic molecules in solutions. Such substances include various groups of drugs transported either to the cathode or anode, namely antibiotics, vitamins, alkaloids, anti-inflammatory, antihistaminic and cardiotropic agents, analgesics, hormonal preparations, etc. Iontophoretic delivery of bioactive formulations is also possible when they associate with electrically charged effective transport units. Naturally, in this situation, it is advantageous to have a non-toxic transport units that can be easily removed from the body after performing their function. These carriers include biodegradable ones (e.g., due to natural metabolic processes), and biocompatible ones, especially those that have their own positive effects on the body. The considered options of iontophoretic drug delivery to the internal organs and lesion foci envisage their preliminary injection (including intracavitary) and external electrodes imposition on the corresponding zone. In view of the above-said, nanoscale systems have significant advantages.

3. Features of skin as a transport medium; transcutaneous transport models

Skin is a very complex biological object that includes many heterogeneous layers that differ in mechanical and physico-chemical properties. The aforementioned layers contain polar (water, inorganic salts), non-polar (lipids, etc.) and amphiphilic (phospholipids, proteins) components. Skin consists of several types of cells which, in addition, are found at different stages of development (keratinization). In addition skin also has pores, hair follicles, blood vessels, and nerves [271–273]. The blood vessels in the skin are arranged as several plexuses found at different depths. There are superficial and deep arterial plexuses and two superficial venous ones. The deep subcutaneous arterial network is located at the subcutaneous fatty tissue and dermis boundary. The superficial (subpapillary) arterial network is located at the base of the papillary layer. Blood is evacuated from the skin capillary network by the papillary venous plexuses and the deep venous plexus, which is located between the dermis and hypodermic tissue [271–275]. Depending on the nature of the transported substance (hydrophilic, lipophilic), different transfer paths predominate. In particular, the question about the main route of substance transfer through the stratum corneum remains controversial [276–278]. Besides, a number of factors, such as skin moisture, lesions, chemical effects, pH, ultrasound, and electric field affect the parameters of transcutaneous transfer [279–287]. All this makes it quite difficult to create an adequate model of transcutaneous substance transfer. Since a model is a simplified representation of a real object, it is important to identify the most relevant skin properties from the point of view of transcutaneous substance transfer. Skin models are conventionally divided into macroscopic and microscopic ones (Table 1). The macroscopic models do not explicitly reflect the specificity of the skin microscopic structure, cell layers geometry, the presence and size of pores, etc. The skin is regarded as a single or multilayer membrane, which is characterized by the corresponding macroscopic parameters (diffusion coefficient, etc.). The microscopic models in turn provide a certain degree of detail when they take into account the skin structure at the micro level (the scale of cell layers and individual cells). Depending on the process type, the substance transfer models are divided into stationary and transitional ones. The stationary models describe a steady process with unchanging concentration profiles of transported substances in the skin, transcutaneous concentration gradients and other parameters of the simulated process. The transitional models characterize the non-stationary processes. One-dimensional (1D), two-dimensional (2D) and three-dimensional (3D) models of transcutaneous transport are distinguished. Their choice is mainly determined by such specific features of the problem as the geometric dimensions of the substance source and, in the case of iontophoresis, of the electrodes,

thickness and transverse dimensions of the skin, direction of concentration gradients and of the electric field. In the case when the transverse dimensions of the substance source significantly exceed skin (membrane) thickness, concentration and electric field gradients are directed perpendicular to the skin surface and all spatial parameters depend only on the coordinate perpendicular to skin surface, the problem can be regarded as one-dimensional. In a number of other cases, two-dimensional models are used, and in certain situations the use of three-dimensional models can be justified. In addition, transcutaneous substance transfer can be enhanced by additional external influences (iontophoresis, phonophoresis, etc.) [286, 287].

TABLE 1. Transcutaneous transfer models

Account of skin structure	Macroscopic	Microscopic
Process type	Stationary	Transitional
Additional impacts	Passive transfer	Iontophoresis, phonophoresis, etc

3.1. Simplified models of passive transcutaneous transfer

In [288], passive transport models are considered as the most simple case of transcutaneous transport. Conventionally, the four most significant processes (Fig. 1) that determine passive transcutaneous substance transfer can be named:

1. Molecular diffusion. The driving force of this process at a specified pressure and temperature is the difference in chemical concentration gradient of the transported substance at the opposite skin boundaries.

2. Separation. According to the Nernst's distribution law the dissolved substance distribution in two practically immiscible phases reaches in some time a value that is characteristic for each dissolved substance and solvent.

3. Metabolism and phase transitions. Examples of such processes are the dissolution, evaporation, cell metabolism and substance removal into the systemic circulation.

4. Adsorption and absorption. Many similar processes can occur in the skin. The binding of a number of substances with proteins (keratin, etc.) can serve as an example.

All the above processes follow the law of mass conservation, which is mathematically expressed by the following equation:

$$\frac{\partial C}{\partial t} + \mathrm{div}\vec{J} = \pi,$$

where C is the substance concentration t is time J is the substance flow and π is the sum of substance sources and sinks.

Diffusion, the first process, is usually described by the first Fick's equation, according to which a substance flow is proportional to its concentration gradient.

$J = -D\nabla C$ where C is the substance concentration, J is the substance flow, D is the coefficient of the given substance diffusion in the given medium.

In a particular case when the area under consideration has no sources and sinks of the substance, i.e., when $\pi = 0$,

$$\frac{\partial C}{\partial t} + \mathrm{div}\vec{J} = 0$$

and, therefore:

$$\frac{\partial C}{\partial t} + \nabla \cdot [-D\nabla C] = 0.$$

The stationary regime can be achieved at constant conditions and only after some time, which is $h^2/6\mathrm{D}$ for the diffusion through a homogeneous membrane, where h is the membrane thickness and D is the diffusion coefficient [279, 287–292]. When several phases are available, as in the case with the transcutaneous substance transfer, the second process, that is, separation should be taken into account. This process is characterized by equilibrium at the boundary of two phases:

$K_{A/B}C_B = C_A$ where $\mathrm{K}_{A/B}$ is the separation coefficient C_A is the substance concentration at the A phase boundary, and C_B is the substance concentration at the B phase boundary.

Metabolism and removal from the system (the third process) are taken into account in term π. If only the processes the rate of which linearly depends on the substance concentration $\pi = q - kC$ occur in the system, then:

$$\frac{\partial C}{\partial t} + \nabla \cdot [-D\nabla C] + kC = q,$$

where k is the process rate constant, which characterizes the amount of substance removed from the system or added into the system per unit of time, and the term q unites sources and sinks that do not depend on the substance concentration. Equations of this type form a system of equations for several substances undergoing mutual transformations. If there are only two substances, then:

$$\begin{aligned} \frac{\partial}{\partial t}C_A^0 + \Delta \cdot [-D_A^0 C_A^0] &= -k_A^0 C_A^0 + k_A^1 C_A^1, \\ \frac{\partial}{\partial t}C_A^1 + \Delta \cdot [-D_A^1 C_A^1] &= -k_A^0 C_A^0 - k_A^1 C_A^1. \end{aligned} \tag{1}$$

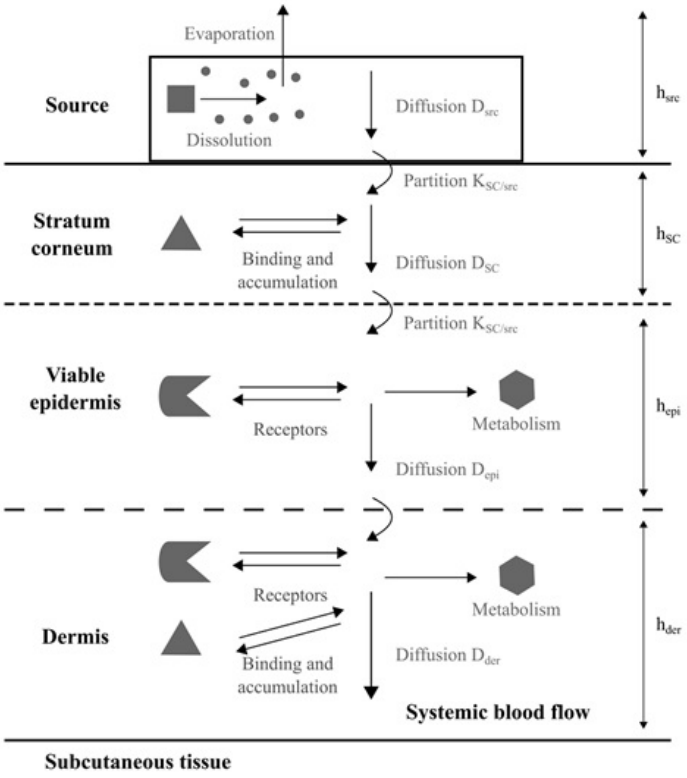

FIG. 1. Diagram of the processes occurring in the skin during the transcutaneous drug administration (based on the diagram from [288])

In this case, both types of particles are transferred by diffusion, however diffusion coefficients are different: D_A^0 and D_A^1. The constants k_A^0 and k_A^1 describe the transformations between the two components. This description of the process is very similar to that of the fourth process, i.e., binding, if C_A^0 and C_A^1 denote concentrations of free and bound substances, respectively. Usually the bound particles are believed to be immobile, that is, $D_A^1 = 0$. It is a reversible adsorption process, the equilibrium condition of which is specified as:

$$k_A^0 C_A^0 = k_A^1 C_A^1. \tag{2}$$

The process is irreversible in the case when any of the constants becomes zero. It should be noted that the above diagram is a simplified one

In order to obtain a linear system of equations, it is necessary to accept several more simplifications. In particular, the role of the binding agent in the binding process is neglected. It is believed that the binding agent is present in excess and its capacity is not limited. Equations (1) describe the general case of binding. In the case of slow binding, the k_A^0 and k_A^1 constants are small and the binding can serve as a limiting stage of the transfer process. In the case of fast binding, the rate constants are large, which makes it possible to further simplify the system. In this case, equations (1) are replaced respectively by equation (2) and the following equation:

$$\frac{\partial}{\partial t}\left(\left(1 + \frac{k_A^1}{k_A^0}\right) C_A^0\right) + \nabla \cdot [-D_A^1 C_A^0] = 0.$$

The description of the processes will not be complete without defining the initial and boundary conditions. Their choice significantly depends on the particular situation. The most frequently accepted initial condition is the absence of a substance in the membrane, i.e., $C(0, x) = 0$ for all x points within the membrane. The ideal sink condition is represented as $C(t, x) = C_{sink} = 0$ for any time instant t and for all points x that are in contact with the ideal sink [277, 288, 293].

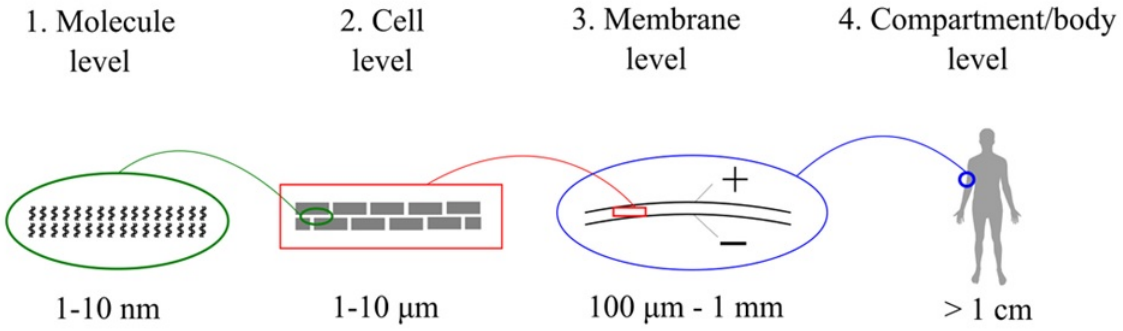

FIG. 2. Levels of detail in transcutaneous transfer models (based on the diagram from [288])

Different levels of skin description can be considered (Fig. 2).

1. Processes at the level of molecules (macromolecules) (1–10 nm), i.e. lipid bilayer level.

2. Processes at the subcellular (0.1 μm) or cellular (1–10 μm) level.

3. Processes at the membrane level (0.1–1 mm), i.e. analysis of the amount of substance that has reached a certain depth in experiments with a diffusion cell.

4. Processes at the compartment/organism level, i.e. the amount of substance that has passed through the membrane in experiments with a diffusion cell or into the body in *in vivo* experiments. Skin layers, as well as the substance source and sink that are seen as peculiar reservoirs are considered as compartments.

The models that describe the transfer process at the 3^{rd} and 4^{th} levels are called macroscopic. They describe the substance source and the skin as a sequence of homogeneous membrane layers (e.g., the substance source/ epidermis/ dermis) through which diffusion occurs. The parameters used in such models are averaged for the corresponding volume (layer, tissue, compartment). The description of the transfer process at the 1^{st} and 2^{nd} levels is done by microscopic models [288].

Thus, it is possible to identify the main classification parameters for the transcutaneous substance transfer models (Table 2). A separate subclass of macroscopic models is represented by pharmacokinetic (compartmental) models [294–296]. The transported substance concentration within one compartment is considered to be uniform throughout its volume. A simple 4 compartment pharmacokinetic model (Fig. 3) was considered as an example in [295] and included the drug source (on the skin surface), the stratum corneum, the viable skin layers, and blood vessels. In this case, each compartment is characterized by two parameters: the substance concentration and its volume. Each stage of the transfer process is characterized by the corresponding first-order rate constant (k_1, k_2, k_3, k_4).

TABLE 2. Main classification parameters for the transport models

Scale of detail	Macroscopic	Microscopic	
Process type	Stationary (established)	Non-stationary (transition)	
Dimension	1D	2D	3D
Additional acting forces	Absent	Electrophoresis, phonophoresis, etc	

The k_1 constant characterizes the drug absorption stage. It is supposed that its value is determined by diffusion through the stratum corneum and the numerical estimate for k_1 can be obtained from the relation D_{SC}/h_{SC}^2, where D_{SC} is the coefficient of drug diffusion in the stratum corneum with h_{SC} thickness. Experimentally, the value of the k_1 constant can be estimated in *in vitro* diffusion experiments on an isolated stratum corneum, including the use of labeled molecules (radioactive, fluorescent labels). The rate constant k_2 characterizes the drug penetration through the skin layers following the stratum corneum, i.e., the viable epidermis layers that contain more water and the dermis

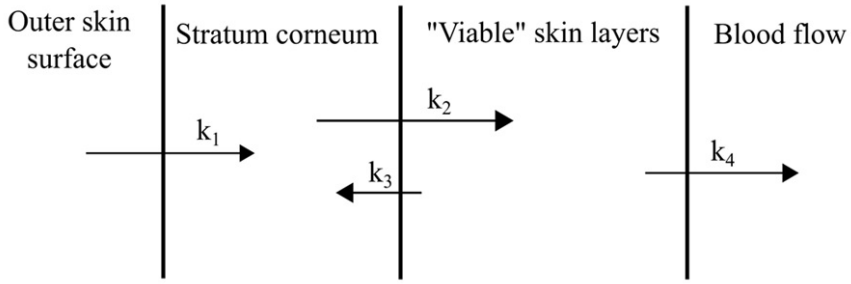

FIG. 3. Compartments in a simple transcutaneous transfer pharmacokinetic model (based on the diagram from [295])

upper part. Its value, by analogy with the k_1 constant, is also associated with the diffusion coefficient related to the square of the diffusion path length, that is D_{VED}/h_{VED}^2, where D_{VED} is the diffusion coefficient in the viable epidermis and dermis, and h_{VED} is the considered skin layer thickness The rate constant k_3 is necessary for taking the effect of accumulation in the epidermis into account; its values are essential for drugs with high lipophilicity (greater affinity for the hydrophobic stratum corneum than for the deeper hydrophilic skin layers). In this model, the drug concentration in the subcutaneous capillaries and the systemic circulation are considered to be the same, so the rate constant k_4 is actually the rate constant of the drug removal from the body. In this formulation, the problem is described by a system of ordinary first order differential equations:

$$\begin{aligned}
\frac{dC_1}{dt} &= -k_1 C_1, \\
\frac{dC_2}{dt} &= \frac{V_1}{V_2} k_1 C_1 - k_2 C_2 + \frac{V_3}{V_2} k_3 C_3, \\
\frac{dC_3}{dt} &= \frac{V_2}{V_3} k_2 C_2 - (k_3 + k_4) C_3, \\
\frac{dC_4}{dt} &= \frac{V_3}{V_4} k_4 C_3,
\end{aligned}$$

where V_i and C_i are the i^{th} compartment volume and drug concentration in it, respectively. The system can be solved analytically; the concentrations in each compartment can be expressed as functions of time [294, 295].

3.2. Improved models of transcutaneous transport

An example of a more complex approach is the hybrid diffusion/pharmacokinetic model suggested in [297] The model diffusion medium is represented by two skin layers; in addition there are two separate areas (compartments) described pharmacokinetically, i.e., the central and peripheral vessels. This model also takes into account binding processes and drug metabolism in the skin. This model is schematically represented in Fig. 4. The introduced drug concentration at the surface of the epidermis stratum corneum is considered constant.

Though the real skin structure is multi-layered, this model treats it as if it consists of two layers. Such a simplification is deemed acceptable, in particular, on the basis of the data presented in [295,296]. It can be then concluded that the epidermis stratum corneum and viable epidermis differ significantly from each other in properties that determine drug distribution. At the same time, the differences in drug distribution between the viable epidermis and dermis are not significant. Thus, it is possible to distinguish two layers: the first includes the epidermis stratum corneum (SC), the second includes the layers of viable epidermis and dermis (usually referred to as VS (from viable skin) or VED (from viable epidermis + dermis). Let's consider the processes taken into account in this model in more detail. The introduced drug undergoes separation at the stratum corneum outer boundary and penetrates into it. It can also become partially bound in the stratum corneum. The binding process in the framework of this approach is described by a double sorption model based on the Langmuir isotherm [298–301]. Furthermore, the drug undergoes separation at the stratum corneum/viable skin boundary. Metabolic processes take place in the viable skin. The $A \to B \to C$ transformation sequence is accepted in the considered model. As a rule, enzyme reactions follow the Michaelis-Menten kinetics, and simple competitive inhibition is also taken into account. B and C metabolites produced in the viable skin diffuse both into the receiving compartment (into the bloodstream) and back into the stratum corneum; this process is described by the first Fick's equation. In general, the rate of reverse diffusion back into the stratum corneum is rather low due to the low diffusion coefficient in the stratum corneum. However, the reverse diffusion is still taken

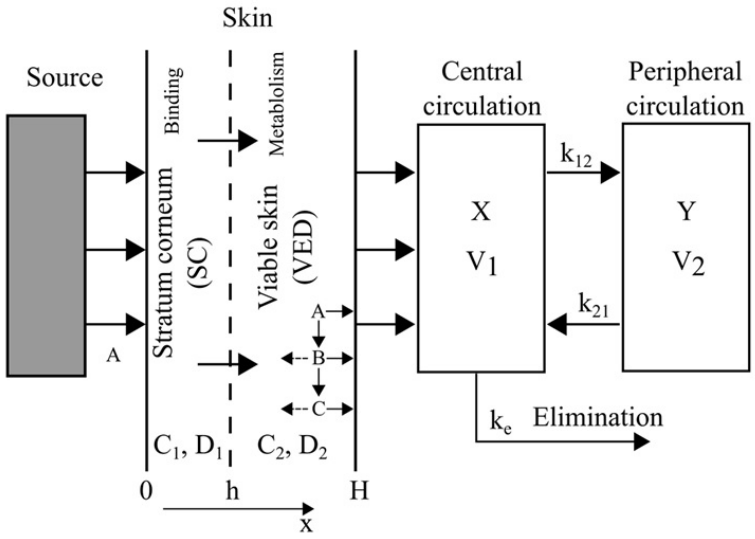

FIG. 4. Compartments in the hybrid diffusion/pharmacokinetic transcutaneous transfer model (based on the diagram from [288])

into account, since it is the stratum corneum that largely determines the drug accumulation in the skin. The drugs that have passed through the viable skin get into such compartments as the bloodstream and tissues. The considered model uses two compartments, and the kinetics of drugs removal from the body is described by the first-order equations. The mass balance of A, B and C metabolites in the skin is described by a system of differential equations:

$$\left(1+\frac{p_a}{(1+q_aC_a)^2}\right)\frac{\partial C_a}{\partial t}=\frac{\partial}{\partial x}\left(D_a\frac{\partial C_a}{\partial x}\right)-\frac{M_aC_a}{B_a+C_a}, \tag{3}$$

$$\left(1+\frac{p_b}{(1+q_bC_b)^2}\right)\frac{\partial C_b}{\partial t}=\frac{\partial}{\partial x}\left(D_b\frac{\partial C_b}{\partial x}\right)+\frac{M_aC_a}{B_a+C_a}-\frac{M_bC_b}{\left(1+\dfrac{C_a}{K_i}\right)B_b+C_b}, \tag{4}$$

$$\left(1+\frac{p_c}{(1+q_cC_c)^2}\right)\frac{\partial C_c}{\partial t}=\frac{\partial}{\partial x}\left(D_c\frac{\partial C_c}{\partial x}\right)+\frac{M_bC_b}{\left(1+\dfrac{C_a}{K_i}\right)B_b+C_b}. \tag{5}$$

Here p and q are the binding rate constants from the double sorption model, C is the substance concentration in the skin, t is time, x is the spatial coordinate, D is the diffusion coefficient, M and B are the Michaelis-Menten kinetic parameters, and K_i is the inhibition constant.

Equations (3), (4) and (5) are applicable both to the stratum corneum ($0 \le x \le h$) without metabolism, and to the viable skin ($h < x \le H$) without binding ($p = q = 0$). At a low substance A concentration, equations (3), (4) and (5) can be reduced as follows:

$$\left(1+\frac{p_a}{(1+q_aC_a)^2}\right)\frac{\partial C_a}{\partial t}=\frac{\partial}{\partial x}\left(D_a\frac{\partial C_a}{\partial x}\right)-k_1C_a,$$

$$\left(1+\frac{p_b}{(1+q_bC_b)^2}\right)\frac{\partial C_b}{\partial t}=\frac{\partial}{\partial x}\left(D_b\frac{\partial C_b}{\partial x}\right)+k_1C_a-k_2C_b,$$

$$\left(1+\frac{p_c}{(1+q_cC_c)^2}\right)\frac{\partial C_c}{\partial t}=\frac{\partial}{\partial x}\left(D_c\frac{\partial C_c}{\partial x}\right)+k_2C_b.$$

Here k are the enzymatic reaction rate constants in the viable skin.

In the general case, the diffusion coefficient is a function of the spatial coordinate (x), time (t) and concentration (C) : $D = f(x, t, C)$. However, this and most other models use the assumption that the diffusion characteristics of the skin do not change during the experiment. Thus, the diffusion coefficient is a function of only the spatial coordinate:

$$D_i=\begin{cases} D_{1i} & (0 \le x \le h; SC), \\ D_{2i} & (h < x \le H; VS). \end{cases}$$

In this case, the diffusion coefficient D should be considered as an effective value due to the heterogeneity of the structure, especially of the stratum corneum. In the general case, the constants k_1 and k_2 of the $A \to B \to C$ enzymatic reactions rate depend on time, which can especially manifest itself in *in vitro* experiments. This dependence may be associated with the processes of enzymes inactivation. In the considered model from [298], it is assumed that the rate constant exponentially decreases with time:

$$k_i = Z_i \exp(-A_i t), \quad i = 1, 2.$$

The rate of drug transfer through the skin can be expressed as:

$$\left(\frac{dQ}{dt}\right)_i = -D_i \left(\frac{dC_i}{dx}\right)_{x=H}.$$

The amount of substance that has transited through a unit of skin area will be expressed as:

$$Q_i = \int_0^t \left(\frac{dQ}{dt}\right)_i dt = \int_0^t \left(-D_i \frac{dC_i}{dx}\right)_{x=H} dt.$$

In the two-compartment model (Fig. 4), the administered drug concentration in the blood plasma will be expressed for the central vessels as:

$$\frac{d(XV_1)}{dt} = \left(\frac{dQ}{dt}\right) S_a + k_{21} Y V_2 - k_{12} X V_1 - K_e X V_1,$$

where X is the concentration in central vessels Y is the concentration in peripheral vessels V_1 and V_2 are concentrations in central and peripheral vessels, respectively S_a is the skin surface area through which the drug is administered.

For the peripheral compartment,

$$\frac{d(YV_2)}{dt} = k_{12} X V_1 - k_{21} Y V_2 \quad [297].$$

The so-called QSPR (quantitative structure-permeation relationship) models are also worth mentioning. This model class cannot be fully attributed to macroscopic or, moreover, to microscopic models. The essence of the QSPR method is in predicting the kinetics of the transcutaneous transfer of a certain substance with a known molecular structure. The prediction is based on statistical analysis of the experimentally determined kinetics parameters for a number of other substances. To this end, large sets of experimental data are used, such as the Flynn's dataset [302–304], which includes data on the transcutaneous transport for 94 substances, and a number of other data sets [305–307]. In recent years, this model class has received a new aid to development thanks to significant progress in the artificial intelligence methods, in particular, in the widespread introduction of the artificial neural networks (ANN) into the practice.

4. Some features of biological target identification systems

The development of modern targeted drug delivery systems includes solving the problems of biochemical target identification in the body. For instance, the so-called homing peptides [308, 309], which, while in the bloodstream and capillaries, can selectively stick to the transformed (tumor) cell membranes. A similar property is demonstrated by compounds of other classes, e.g., the water-soluble folic acid (B9 vitamin) and some other substances. At the same time, the homing peptides can transport bioactive substances associated with them, or chemotherapy drugs. When conjugation of homing peptides with quantum dots occurs, accumulation of the latter in the tumor region and its luminescent diagnostics using primary IR radiation, as well as dynamic laser therapy become possible. There exists a problem of quantum dot toxicity for the organism, in particular, of those based on nanoparticles of transition metal chalcogenides. The protective shell function for toxic quantum dots with a transition layer between the chalcogenide and peptide molecules can be performed by the above-mentioned biocompatible PEG polymer. The possibility of targeted, homing peptide-assisted transport to and accumulation in the tumor area of magnetic particles, which further exert therapeutic effect through hyperthermia, cannot be excluded. The presence of transport units that are mobile in the electric field and carry drug molecules or ions does not exclude the combination of such units with homing peptides, folic acid and other bioactive molecules with affinity to certain cell membranes. Potentially, it makes it possible to create a drug, the transport units of which can be controlled by an electric field, as well as selectively adhere to the transformed cells. The drugs (conjugates) that include folic acid can be absorbed together with their contents by the cells through endocytosis.The so-called receptor-mediated endocytosis that employs various kinds of protein vectors (hormones, enzymes, specific peptides, antibodies, glycoproteins, glycolipids, and viruses) occupies a significant place in ongoing studies worldwide [310–323]. Drugs bind to protein vectors by molecular linkers. The autologous blood cells, such as leukocytes and erythrocytes, are used as carriers for targeted delivery. The undoubted

advantage of the carriers in the latter case is their complete biological compatibility, the body's ability to utilize such "containers". Among the disadvantages is a relatively large volume of carriers that are not always able to penetrate tissues to biological targets. In addition to the delivery of drugs to the cell surface, intracellular targeted drug transport systems are being developed [324–328]. The matter is about an even more precise hitting the specified compartments directly in cells of a certain type by the nominal transport units.

5. The possibilities of using nanocluster polyoxometalates for the bioactive substances delivery

5.1. The structure and properties of molybdenum-containing polyoxometalates

Molybdenum can form a large number of different compounds; it belongs to the structural elements for polyanions. The ability of oxygen-containing molybdenum compounds to condense and form nanocluster polyoxoanions is due to its properties, such as the relatively large radius of Mo^{6+} cation (0.062 nm according to Pauling) [329], which allows it to have a coordination number of 6 in oxygen-containing compounds, as well as 7 (pentagonal bipyramid of oxygen atoms). For comparison, the Cr^{6+} cation with a radius of 0.052 nm [329] has a coordination number for oxygen equal to 4. The second property that determines the ability of oxygen-containing molybdenum compounds to form nanoclusters is that molybdenum is a good acceptor of oxygen electrons. The relatively simple oxygen-containing molybdenum compounds are, for instance, MoO_3, Mo_5O_{14}, and $Mo_{17}O_{47}$. In the last two compounds, molybdenum is simultaneously found in two oxidation states (5+ and 6+). The behavior of oxygen-containing molybdenum ions in solution depends on the conditions: for example, molybdic acids with the general formula of $H_xMo_{y(6y+2x)/2}\cdot H_2O$ dissociate in an aqueous medium in different ways, depending on the medium's acidity. In the case of acid-type dissociation, the end product is the molybdate ion. Polymerized and protonated molybdates can be regarded as intermediate products. Since acid-type dissociation is a reversible process, molybdate acid solutions represent a complex system of various molybdenum ionic species. The basic-type dissociation yields molybdenyl ions.

Polyoxometalates (POM) is a class of inorganic compounds that represent by themselves multicenter anionic groups of transition metals, which also include oxygen atoms and, quite often, some other elements. POM nanoclusters are a vast array of complex compounds, the structural blocks of which are polyoxometallate molecules. Molybdenum is one of the elements that can form POM nanoclusters, namely polyoxomolybdates. The initial components for polyoxoanion nanoclusters are molybdate or heptamolybdate ions. These compounds are considered as promising materials in many scientific and applied fields, in particular, as catalysts for fine organic synthesis of the so-called templates for creating composite structures. There are indications of the possibility of POM application in biomedicine. For instance, their anti-cancer activity was reported in [330, 331], especially for the compound $[NH_3Pri]_6[Mo_7O_{24}]\cdot 3H_2O$ (isopropyl ammonium heptamolybdate, designated as PM-8) in the examples with breast cancer, sarcoma and adenocarcinoma. PM-8 is water soluble; its structure is preserved in aqueous solutions at pH 5–7. POM can be isolated in the form of metal-ammonium or organometallic salts. A study on mice with tumors showed that some POM, such as PM-8, PM-17, PM-26 and PM-32, show anti-cancer activity against human cancer. It was also reported that $[NH_4]_6[Mo_7O_{24}]\cdot 4H_2O$ and $K_6[Mo_7O_{24}]\cdot 4H_2O$ were found to be effective, while $[NH_3Pri]Cl$ ineffective against mouse sarcoma. A particularly noticeable suppressionn of the sarcoma growth was demonstrated by PM-8. According to the results the polyoxoanionic structure of Mo_7O_{24} is crucial for the anticancer activity [331]. From the point of view of biomedical application, the use of POM as part of complexes based on them seems to be promising. Reference [332] describes the creation of a number of conjugates of biological substances and organic compounds with a POM with the Anderson structure and the formula $MnMo_6O_{18}[(OCH_2)_3CNH_2]_2^{3-}$, which has a proven antitumor effect. Among the above-mentioned organic compounds are the cholic dehydrocholic and adipic acids; cholesterol, and diacetone-D-galactose (pretreated with succinic anhydride to obtain derivatives containing the carboxylic group). These substances are selected from the group of identifier molecules specific to certain tissues or cells. It was demonstrated in the paper that the correct choice of ligands can ensure a synergistic effect. Thus, the best result was achieved when a POM cluster was conjugated with cholic and dehydrocholic acids. Such conjugates demonstrated an increased antitumor activity and selectivity in comparison with the initial cluster and ligands [332–334].

Among the most interesting types of POM nanoclusters are the spherical polyoxomolybdates with a fullerene-like structure, which are called Keplerates. These POM were discovered by the research group of Prof Achim Müller [335]. The first obtained POM nanocluster contains 132 molybdenum atoms (Mo_{132}), of which 72 have an oxidation state of 6+, and 60 of 5+. Molybdenum oxygen polyhedra that form Keplerates are octahedral configurations and pentagonal pyramids connected by edges and tops (Fig. 5) Such compounds are stabilized by ligands (in particular, acetate groups) and water molecules. Compounds belonging to the class of Keplerate-type POM nanoclusters attract attention both by the uniqueness of their structure and by the relative simplicity of their synthesis [336]. Their formation occurs through self-assembly from the initial molybdenum compounds under the conditions of medium acidity regulation and in presence of a specified amount of reducing agent. POM show stability in weakly acidic solutions, and can be isolated

in crystalline or amorphized state. Due to the presence of an internal cavity and pores in the structure of Keplerates, it is possible to introduce various substances inside them, both ions and molecules [337, 338], including bioactive substances, which makes them promising in the context of creating nanocapsules for targeted drug delivery [339]. Fig. 5 shows structure of a POM with pentavalent molybdenum replaced by iron(III) ions in the initial Mo_{132} cluster. The absence of toxic Mo(V) in its structure and its electron-transport properties [340] make this compound particularly interesting. It has the following chemical formula: $[Mo_{72}Fe_{30}O_{252}(CH_3COO)_{12}\{Mo_2O_7(H_2O)\}_2\{H_2Mo_2O_8(H_2O)\}(H_2O)_{91}] \sim 150H_2O$ and its common abbreviation is $Mo_{72}Fe_{30}$ [341]. In dilute aqueous solutions or at an increase in the medium pH, the POM clusters decompose over time into simpler compounds [342, 343]. $Mo_{72}Fe_{30}$ decomposes into compounds that are relatively harmless to the body. Toxicity studies did not reveal any significant adverse effect of $Mo_{72}Fe_{30}$ on the animal subjects [344]. Studies of the acute and subacute effects of $Mo_{72}Fe_{30}$ on the functional status of such organs of experimental animals as the liver, kidneys, and pancreas, confirmed the absence of appreciable negative effects [345, 346]. In addition, the available experimental data on the effects of $Mo_{72}Fe_{30}$ on liver and blood cells [347] suggest that this nanocluster does not cause the autoimmune reaction of lymphocytes to hepatocytes. POM and products of their destruction showed no prolonged accumulation in the body.

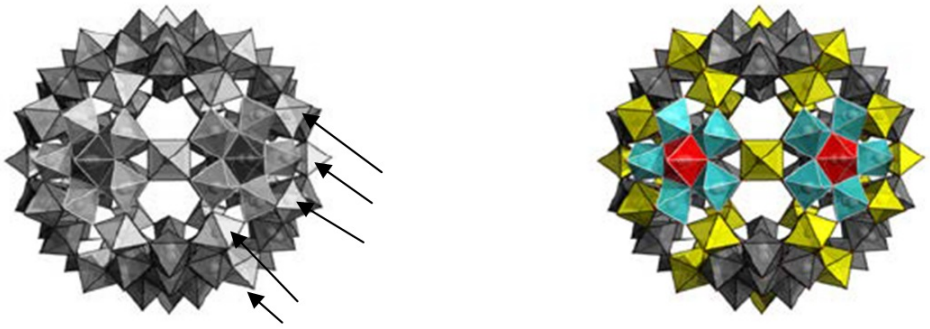

FIG. 5. Schematic representation of the POM $Mo_{72}Fe_{30}$ structure (adapted from [353])

The positions of some oxygen polyhedra belonging to iron ions are shown by arrows (such polyhedra are highlighted yellow in the electronic version of the paper) One of the above-mentioned octahedra is located directly in the center of the structure.

In aqueous solutions $Mo_{72}Fe_{30}$ is known to exhibit the properties of a weak acid, that is, it partially dissociates to form negatively charged polyanions with the maximum charge of 22- [348]. Since the $Mo_{72}Fe_{30}$ nanocluster exists in solution in the ionized form, its movement can be controlled by means of an electric field, and therefore, its introduction into the body by iontophoresis is possible. For instance, *in vitro* and *in vivo* experiments (on rats) have demonstrated that $Mo_{72}Fe_{30}$ is transferred through the skin under the action of an electric field of the corresponding polarity more rapidly than during passive transfer [349–351]. The electrophoretic (iontophoretic) drug administration method has several advantages compared with injection methods of administration, e.g., non-invasive nature of the procedure, i.e., no disruption of the body's natural barriers during the procedure; a possibility to have a predominantly local impact, and to achieve a prolonged action due to the creation of a drug depot in tissues, etc. A weakness of the method is the significantly limited rate of drug administration compared with the injection methods. The results of studies on the possibility of using $Mo_{72}Fe_{30}$ for transporting bioactive substances are given below. It should be noted that the organic part of the molecules in the considered POM does not contain toxic components, while iron and molybdenum are essential microelements that are necessary for the body as components of the vitamin-mineral complexes involved in the blood production, enzymatic reactions and other important biological processes [352].

5.2. Transport characteristics of polyoxometalates: modeling and experimental study

The first data on the transport properties of POM $Mo_{72}Fe_{30}$ and Mo_{132} were obtained with regard to their pure aqueous solutions, in particular, in the case of capillary electrophoresis. The diffusion coefficient for Mo_{132} and $Mo_{72}Fe_{30}$ ions in water was $1.8 \cdot 10^{-7}$ cm^2/s (at a concentration of $4 \cdot 10^{-4}$ mol/l) and $7.3 \cdot 10^{-7}$ cm^2/s (10^{-5} mol/l), respectively [342, 354]. The magnitude of the electrical mobility of these ions was similar and amounted to $6.4 \cdot 10^{-8}$ m^2/V·s. The reference [340] offers data on the specific and ionic conductivities of the considered POM solutions; the values of ionic conductivity at infinite dilution for $Mo_{72}Fe_{30}$ and Mo_{132} were 6 and 14 S·m^2 mol^{-1}, respectively. The number of POM polyanion transfers in aqueous solutions is estimated at 10–20%. The obtained

data showed ion mobility to be sufficient for transport purposes. This made it possible to proceed to the next stage of research, i.e., the study of the POM transcutaneous electrical transport.

POM anions transcutaneous transport was modeled *in vitro* using native skin samples and also studied *in vivo* [339, 349]. The obtained data made it possible to evaluate the diffusion coefficient for $Mo_{72}Fe_{30}$ through the studied membrane; the average value of which was $1.8\pm0.2\cdot10^{-11}$ cm^2/s, and the calculated electrical mobility was found to be $5.5\cdot10^{-10}$ m^2/(V·s). Under the action of an electric field, the diffusion flux of Keplerate ions through the dermal membrane increased, at least by an order of magnitude, and was quite acceptable for practical use. In contrast to the above-described experiments, which showed the absence of long-term accumulation of POM in organs and tissues after intravenous, intramuscular, or oral administration, transcutaneous transport experiments resulted in temporary drug accumuation in the skin, which was confirmed by the analysis of skin thin sections obtained after POM electrophoresis and sample freezing in liquid nitrogen [355]. The analysis (Fig. 6) was performed by the X-ray fluorescence method. The content of iron, reflecting the concentration of POM after the electric transport of $Mo_{72}Fe_{30}$, was significantly higher than in the intact sample. The POM content in the skin has its maximum, which confirms the possibility of accumulation [351], localized in the region preceding the zone of the maximally dense capillary network (Fig. 6), through which the enhanced POM outflow into the circulatory system is possible. The difference in absolute values of POM concentration in two parallel experiments may be due to the individual characteristics of the biological objects, i.e., of the native membranes taken for the experiments. The relatively low POM concentration in the skin's upper layers is determined by the fact that the epidermis that contains little water, does not accumulate, as a rule, the injected substances that travel through its pores.

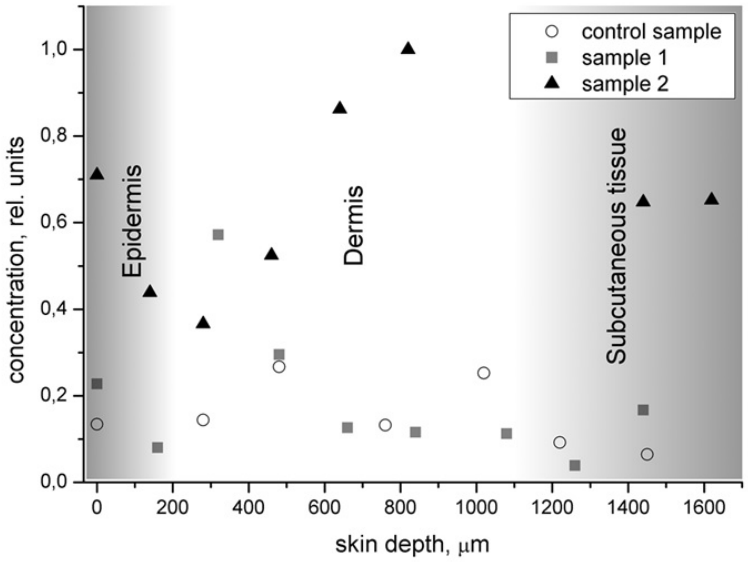

FIG. 6. The distribution of iron, a POM component, within skin depth [355]

After confirming the principal possibility to transport Keplerates electrophoretically through the isolated skin, their diffusion was investigated in an *in vivo* experiment [349]. Of interest are the results indicating an increase in the ability of POM to penetrate the skin during iontophoresis when they are components of some ointments used to increase skin permeability. For instance, the content of POM components in the blood plasma increased about three-fold 1 hour after the procedure that used a silicone-based ointment (gel), while the silicon-titanium-containing glycerogel did not yield such an effect.

Experiments were conducted to select the parameters of iontophoretic procedures, and the current-voltage characteristic of the electrode system [355] (Fig. 7) was obtained, when lead or lead-tin alloy electrodes were separated directly by the native skin membrane. Upon reaching the applied voltage of 4 V, the current reached its maximum and then dropped due to the anodic passivation of the electrode material. That is why 4 V was chosen as the optimal operating voltage. The study of polarization phenomena on the skin membrane has shown that they are capable of reducing the effective value of the electric field acting on the transported ions. The potential difference was measured in the original cell on different sides of the membrane using additional electrodes placed in close proximity to the skin, with a voltage of 4 V applied to the working electrodes (Fig. 8). The cathode part of the cell was filled with the

$Mo_{72}Fe_{30}$ solution (0.5 g/l, or 2.68^{-5} M). In presence of pure water on the anode side of the membrane, polarization of the initial concentration occurred and counteracted the applied field, however it gradually decreased with the penetration of a part of ions across the membrane. This case models electric transport into such media of the body where the dissolved ions concentration is low. When the anode space of the cell contained cattle blood serum, then such polarization did not occur initially due to the presence of ions with different signs in it, like in the electrolyte, but increased as the electrophoresis proceeded, because POM anions are much less mobile than, e.g., metal cations found in the serum. The local maximum on this curve may be due to the accumulation and release from the membrane of a component of a complex system that contains biological materials. The obtained data can be used when modeling processes and calculating the parameters of electrotransport in native membranes.

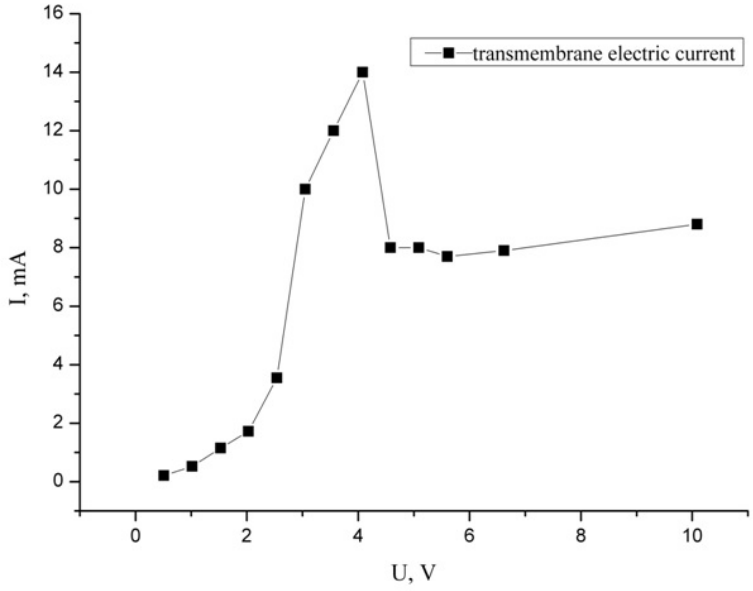

FIG. 7. Volt-ampere characteristic of the electrodes/skin membrane system [355]

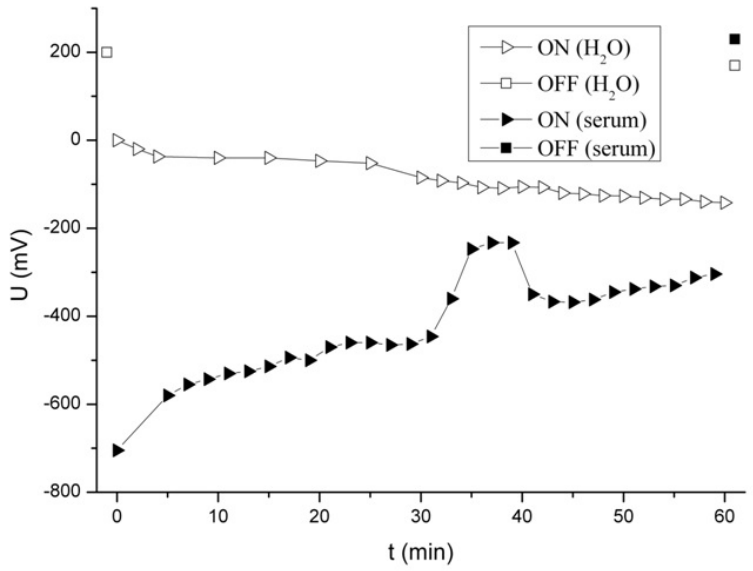

FIG. 8. Skin membrane polarization with water or blood serum in the anode space, with the field on and off [355]

The correctness of parameter choice for the iontophoretic effect was verified in [349] using the level of glucose in the blood of animals as a non-specific indicator of a stressful situation. The level of glucose did not increase

during iontophoresis in comparison with this indicator in intact animals (Table 3), which means that they did not experience strong discomfort. The experiment did not detect significant changes in the indicators characterizing the functional state of the heart, liver, kidneys and pancreas, which indicates the absence of a pronounced toxic effect from this method of POM administration. The $Mo_{72}Fe_{30}$ concentration in the iontophoretic solution was 1 mg/ml. The molybdenum and iron content determined in plasma and skin are presented in Table 4. The introduction of POM by iontophoresis contributed to an increase in the molybdenum content in the blood by almost 8 times, and by 4.2 times in the skin, thus indicating effectiveness of the technique and the possibility of POM transport into the body *in vivo*.

TABLE 3. Animal blood plasma biochemical indicators 1 hour after a single iontophoretic introduction of the iron-molybdenum POM

Indicator	Group of animals	
	Intact	After iontophoresis
Glucose, mmol/l	6.9±0.1	6.7±1.0
AST, U/l	13.2±0.7	13.5±1.2
ALT, U/l	9.1±0.5	11.3±1.2
AST/ALT	1.46±0.10	1.22±0.18
Alkaline phosphatase, U/l	50.4±3.0	51.2±7.1
Alpha-amylase, mg/s·l	29.7±2.9	33.9±6.5
Total protein, g/l	72.0±2.7	71.4±1.5
Creatinine, μmol/l	65.8±6.2	57.3±1.2

AST – aspartate aminotransferase;

ALT - alanine aminotransferase

TABLE 4. Mo and Fe content in the skin and blood plasma before and after iontophoretic introduction of the iron-molybdenum POM

Group	Mo, μg/l		Fe, μg/l	
	Skin	Plasma	Skin	Plasma
1 – intact	2.3±1.0	11.6±2.9	30.0±0.1	73.3±0.1
2 – electrophoresis	9.7±1.*	89.3±0.3*	208.0±0.7*	53.5±0.3*

* – differences from the intact group are significant with the error probability $P < 0.05$

The *in vivo* experiments have shown the possibility of iontophoretic transfer of ionic $Mo_{72}Fe_{30}$ associates with lanthanum [350], when the positively recharged complexes moved to the cathode instead of anode. The observed simultaneous increase in concentration in the skin of all three elements (iron, molybdenum, lanthanum) during the transport from the anode to cathode is possible only if the associate is transferred as a whole. The absence of a significant increase in the molybdenum and iron concentration in the muscle tissues immediately after iontophoresis, as well as the oppositely directed change in the content of these elements in the deep muscles one hour after the procedure, along with an increased content of lanthanum there, suggest that the transferred ion species dissociates after passing through the skin barrier and its components get carried away by the bloodstream. In this case, the POM-transferred drug should be released in the area adjacent to the electrophoresis area. It is important to note that the lanthanum/molybdenum mass ratio determined in the obtained keplerate-lanthanum associate, is about 0.8. The value of this indicator in the skin of animals immediately after iontophoresis, taking into account the content of elements in the skin of intact animals, is about 0.79, which almost coincides with the original value.

The $Mo_{72}Fe_{30}$ transfer through the skin was theoretically modeled in [351]. The basic initial data for modeling the POM transfer process were taken from the results of experiments from [349] performed in the absence of a difference in potentials and with the application of an electric field, which show an increase in the POM concentration during the observation time (45 minutes). According to the data obtained without the electric field application, the coefficient of the POM diffusion through the studied membrane was estimated by the formula:

$$D = \frac{\Delta m}{S \cdot \Delta t} \cdot \frac{\Delta x}{\Delta c},$$

where Δx is the membrane thickness, Δc is the difference in Keplerates (POM) concentrations in the upper and lower solutions, and Δt is time period. The time-averaged value of the coefficient of POM diffusion through the skin membrane (1.77±0.20) 10^{-11} m^2/s was obtained and further used in numerical calculations using the proposed model. Experiments involving the electric field action also made it possible to estimate the POM electric mobility.

A model of the POM transfer through the skin membrane as a porous medium was considered. The model of a porous medium employed the expressions for the diffusion (D index) and external electric flows (E index), which take into account their mutual influence:

$$J_D = -D\frac{dc}{dx} - \mu c(x)\frac{\partial \varphi}{\partial x}, \quad J_E = -\alpha\frac{\partial c(x)}{\partial x} - \gamma\frac{\partial \varphi}{\partial x}, \tag{6}$$

where $c(x)$ is the diffusing particles concentration ([c]=mol/m^3), D is the free diffusion coefficient ([c]=mol/m^3), α is the unknown coefficient that further requires determination ([α]=A·m^2/mol), γ is the medium electrical conductivity coefficient ([γ]=1/m·Ohm), μ = q_iD/RT_0 (the Nernst-Einstein relation), a quantity characterizing particle mobility in an electric field ([μ]=A·m^2/J), R is the universal gas constant ([R]=J/K·mol), and T_0 is the absolute temperature. When deriving the equation and performing calculations, the dependence of the electrical conductivity (γ) on the POM concentration (c) was taken into account. The experimental value of μ was 1.50·10^{-8} m^2/(V·s). It was established that under the action of an electric field, the diffusion flux of POM ions through the skin membrane increased at least by an order of magnitude, as is already indicated above. According to the Onsager's principle of cross-coefficients symmetry, $\alpha = \mu RT_0$. Using the thermodynamic approach [356, 357], a differential equation was obtained for the POM concentration in the membrane:

$$\frac{\partial c}{\partial t} = D\frac{\partial^2 c}{\partial x^2} + \mu\frac{\partial c}{\partial x}\frac{\partial \varphi}{\partial x} + \frac{c}{RT_0}\left(\frac{\partial \varphi}{\partial x}\right)^2\left(\frac{\partial \gamma}{\partial c}\right). \tag{7}$$

The derived equation shows that there is a weak spatial heterogeneity of the concentration gradient in relation to the total POM concentration in the membrane. This one-dimensional diffusion equation was used in numerical calculations, taking into account the initial and boundary conditions, as well as the dependence of the specific electrical conductivity of the membrane on the concentration. This equation describes the POM diffusion, taking into account the influence of the electric field φ. To solve the equation (7) numerically, the following basic assumptions were used. The direct POM accumulation can occur only in the epidermis, since the dermis and papillary layer are permeated by a large number of blood vessels that contribute to the spreading throughout the body of the particles, which have passed through the upper layers of the skin. Therefore, the POM concentration at the lower boundary of the skin is $c(l) = 0$. Due to the relative smallness of the diffusion coefficient, it can be assumed that the concentration of the POM solution on the outer surface of the skin is constant (i.e., $c(0)$=const). The numerical calculation of equation (7) was performed using the implicit difference schemes method widely used in various fields of science [358–362].

Thus, the transcutaneous POM transfer into the body was mathematically modeled. The experiments on the POM iontophoretic transport into animals [350] have shown that the content of molybdenum after iontophoresis in the muscle tissue layers adjacent to the skin is significantly lower than in the skin. A Keplerate accumulation is formed in the skin, while the POM that reached its inner boundary are intensively transported away via the bloodstream. A mathematical model of the dependence of the POM concentration distribution within the skin layer on the time and membrane thickness was used to perform numerical calculations for the conditions when a voltage of 4 V was applied, and the distance between electrodes was 2 cm at T_0=300 K. The experimentally estimated values of the diffusion coefficient (D=1.77·10^{-11} m^2/s) and of mobility (μ=1.50.10^{-8} m^2/V· s) were used in this case. In equation (7), the term with the derivative ($\partial\gamma/\partial c$), i.e., the dependence of the specific electrical conductivity on the concentration, remained unknown; therefore, it was set empirically as a power function $\gamma = ac^b$. The values calculated for the constants a and b were found to be 1.10^{-14} for a, and -2.2 for b. These parameters were determined taking into account the experimental value of the coefficient of POM diffusion through the skin membrane. Based on the calculations using equation (7), POM concentration profiles in the skin after switching the electric field on were built (Fig. 9a). A theoretical prediction showed that POM accumulation can occur near the upper boundary of the skin layer.

An increase in the POM concentration in the membrane (Fig. 9a) over time and its drop with the advance deeper into the skin may be due to a strong POM outflow from the inner boundary (the anode space). In this case, a sharp

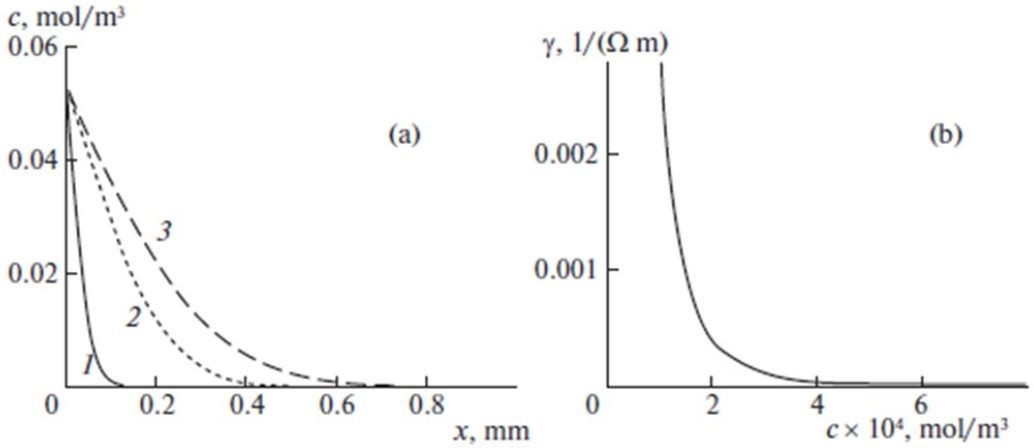

FIG. 9. a) POM concentration as a function of variable x (skin thickness), which varies within the limits $[0; l]$ (l is the skin layer thickness, $l = 1$ mm): curve 1 – 50 s; 2 – 150 s; 3 – 1800 s; b) Dependence of the POM specific electrical conductivity on the concentration (c) in the membrane [351]

increase in the POM concentration in the upper layer of the membrane already at the initial moments of time, accompanied by a decrease in electrical conductivity to the minimum values (Fig. 9b), leads to the situation when further on the penetration of POM into the membrane proceeds due to chemical diffusion, and this fact indicates the formation of a POM depot in the membrane.

The concentration profiles helped to determine the coefficient of POM diffusion in the skin. By using the inclination angle tangent ($\tan\alpha$) for the dependence of $\ln(C)$ on x^2, the diffusion coefficient D was determined according to the formula $D = 1/(4t \cdot \tan\alpha)$, where t is the current time, to which the spatial concentration profile taken for evaluation corresponds. The diffusion coefficient D value of $1.5{\cdot}10^{-11}$ m^2/s obtained by numerical calculations is close to the experimental $D = 1.77 \cdot 10^{-11}$ m^2/s, which proves the adequacy of the proposed mathematical model of POM transport in a membrane. The calculated data correlated well with the experimental concentration profiles (Fig. 6) of POM distribution within the skin thickness, which also confirmed the conclusions made. Thus, the possibility of intensifying the process of iontophoretic transcutaneous POM transfer is shown by an increase in the transferred flux by an order of magnitude compared with self-diffusion. In principle, this confirms the possibility of creating an effective system for the delivery by POM of the associated bioactive substances. The created model contains the empirical dependence of the coefficient of POM specific electrical conductivity in the membrane on the concentration, which allows the evaluation of the membrane electrical conductivity.

The use of the technique developed in [363] demonstrates the ability of POM to increase the permeability of cell membranes for drugs, e.g., antifolate cytostatic agents. It is important for potential use in oncology and requires further research [364,365]. To study the influence of $Mo_{72}Fe_{30}$ on the transport of cytostatic into the cells, *Drosophila melanogaster* flies were used at the pupa and larva early and late embryogenesis stages, and aminopterin was used as a model drug, the increased effect of which in the presence of POM indicates the potential reduction of the therapeutic doses to be used.

5.3. POM-based transcutaneous transport of associates

Proceeding from the results of studies on the association of POM with bioactive substances and the possibility of organic substances retention in the internal cavity and external sphere of POM [366], experiments were conducted and demonstrated that it is promising to use the electrophoretic (iontophoretic) transcutaneous transport of the resulting associates (conjugates). The possibility of efficient transport of the bioactive substances with POM has been experimentally confirmed [367]. The *in vitro* experiments showed the electric field-stimulated transfer of $Mo_{72}Fe_{30}$ associated with thiamine chloride as a model substance. Also, the transcutaneous transfer of the POM-associated insulin was demonstrated; moreover, insulin retained biological activity [367], as its concentration in the trans-membrane space was measured by enzyme immunoassay.

The described experiments yielded an estimate of the effective coefficients of the conjugates diffusion concerning thiamine and POM, which were $6.79{\cdot}10^{-12}$ and $1.04{\cdot}10^{-11}$ m^2/s, respectively. For pure POM, the values of D in these conditions ranged from $1.02{\cdot}10^{-11}$ to $2.14{\cdot}10^{-11}$ m^2/s (the spread of D values may be due to the individual characteristics of skin samples obtained from different animals). However, in general, the coefficient of $Mo_{72}Fe_{30}$

diffusion in the presence of thiamine chloride does not differ much from D of pure POM. To calculate the value of D, some approximations were assumed for a single-layer homogeneous membrane. The electric field inside the membrane was considered uniform. The potential difference applied to the electrodes and the distance between the contacts allowed estimation of the field intensity. The diffusing particle concentration in the initial solution was considered constant. The concentration in the trans-membrane solution was assumed to be zero. In such an approximation, the process of electrodiffusion of the charged particles (in particular, of POM particles) obeys the Nernst–Planck equation [351]. The Nernst-Planck equation was solved numerically.

The results of *in vitro* iontophoretic experiments that were performed at room temperature and involved $Mo_{72}Fe_{30}$ associates with polyvinylpyrrolidone in a 160:1 molar ratio between the polymer monomolecular units number and POM showed a possibility of their transport through the skin. Estimates of the increase in the concentration of associate components (molybdenum and iron) in the anode space over time (the maximum duration of each experiment was 45 min) made possible the determination of the effective diffusion coefficient D for POM. The estimated diffusion coefficient value was $7.34{\cdot}10^{-13}$ m^2/s in the experiments The reduced mobility of associates in the skin as compared to pure POM is due not only to the increase in the size of formations (aggregates). It may be assumed that it was mainly caused by the fairly active interaction of the polymeric shell with the protein components contained in, e.g., cell membranes, and, apparently, with the phospholipid part of these membranes with the outward-facing polar moieties. Fairly strong interaction between polyvinylpyrrolidone and proteins was shown in particular in [368], and also there were indications of the interaction of other water-soluble polymers with molecules in the media of the body [369]. On the other hand, the formation of POM $Mo_{72}Fe_{30}$ associates with polyvinylpyrrolidone is thermodynamically beneficial [370], as is noted above. These two factors seem to contribute to the slowing down of the POM associate movement in the skin and creation of a depot. In this relation it should be noted that a significant role in the transport and conjugation properties of both nanoscale particles in general and POM in the body's media is played by their ability to form associates with proteins [371–377]. Proteins form a peculiar crown on the nanoscale particles, which largely determine the behavior of the latter in the body, their interaction with albumins, globulins and other proteins in the blood serum, in particular, POM stabilization [372].

6. Conclusion

An analysis of the information available in the literature taking into account the historical aspect of the development of fundamental and applied research in the field of targeted drug delivery, permits one to draw the following conclusions. The development of modern means of targeted delivery follows the way of creating hybrid nanocompositions, including those that contain organic and inorganic components. The hybrid systems can combine the functions of diagnosis and treatment of the affected organs and tissues. They include components that serve to identify biological targets, as well as to actively influence the affected areas due to the local release of drugs, or to photo- and magnetodynamic effects. Significant progress has been achieved in the use of such means of targeted delivery, including liposomal methods. Attention is paid to exploring the possibility of expanding the practical application of the carbon material-based therapeutic agents, such as buckyballs (fullerenes), graphene, carbon nanotubes, nanodiamonds, etc. An important aspect of the research and practical implementation is the study of the properties of metal, oxide and other inorganic nanosized particles, including those with magnetic, luminescent properties, which can have their own bioactivity, as well as be used as part of diagnostics and photo- and magnetodynamic therapy methods. Technologies for obtaining nanoscale particles with specified characteristics, adapted for the formation of nanocompositions, are being actively developed. The use of magnetic particles makes possible their delivery and localization under the action of the corresponding fields, or magnetic hyperthermia. The systems of targeted delivery with the electrically charged particles can be used for efficient transport, including transcutaneous, under the action of an electric field. The use of nanocomposites in biomedicine is associated with the development of shells consisting, in particular, of polymeric components (dendrimers, block copolymers, natural biocompatible polymers, proteins, lipids, etc.), as well as with the inclusion of targeted delivery vectors, including intracellular (proteins, antibodies, nucleic acids, etc.). Much attention is paid to the possibility of developing harmless biocompatible composite means of targeted delivery.

For the effective use of the above-mentioned means of transcutaneous drug transport, model representations have been developed for predicting the delivery processes. Models for the means of transport for targeted delivery take into account special properties of nanostructured objects and real skin as a transfer medium to a varying extent, which, in one way or another, complicates the setting of boundary conditions and calculations using such models, but increases reliability of calculations. The models of the means of targeted delivery transportation are continuously improving.

Nanocluster polyoxometalates, in particular those based on molybdenum compounds, possess properties that make it possible to consider them among other means of targeted delivery. For instance, some polyoxometalates have their own bioactivity, for example, their anticancer activity has been detected. On the other hand, there exist water-soluble polyoxometallates that are practically non-toxic to the body of warm-blooded animals and can form multiply

charged anions that are able to associate with protein molecules, polymers and drugs. The model and experimental studies have shown the possibility of effective transdermal iontophoretic transport of drugs as part of conjugates with polyoxometalates. Such polyoxometalates include the iron-molybdenum compound $Mo_{72}Fe_{30}$ with the keplerate type structure, which has, among other things, an internal cavity and pores that link it to the environment. On the one hand, this compound and its components do not accumulate in the body for a long time; while on the other hand, Keplerates are capable of accumulating in the skin, which can be used for the prolonged drug action. In addition, this polyoxometallate increases the cell membranes permeability for cytostatics (experiments were performed on insect larvae), which, in principle, allows a reduction in the therapeutic dose of such drugs. It is of interest to further study nanocluster polyoxomolybdates with keplerat-type structure as a basis for new promising systems for targeted delivery of bioactive substances and actual therapeutic agents.

Acknowledgements

The paper was prepared in the framework of implementation of the state assignment from the Ministry of Education and Science of the Russian Federation (Projects Nos. 4.6653.2017/8.9 and AAAA-A18-118020590107-0), and of the Program for Increasing Competitiveness of UrFU (Agreement No. 02.A03.21.0006).

References

[1] Holgado M.A., Martin-Banderas L., Alvarez-Fuentes J., Fernandez-Arevalo M., Arias J.L. Drug Targeting to Cancer by Nanoparticles Surface Functionalized with Special Biomolecules. *Curr. Med. Chem.*, 2012, **19**(19), P. 3188–3195.

[2] Parashar A.K., Kakde D., Chadhar V., Devaliya R, Shrivastav V., Jai U.K. A review on Solid Lipid Nanoparticles (SLN) for controlled and targeted delivery of medicinal agents. *Curr. Res. Pharm. Sci.*, 2011, **1**(2), P. 367–47.

[3] Ventola C.L. Progress in Nanomedicine: Approved and Investigational Nanodrugs. *Pharm. and Therapeutics*, 2017, **42**(12), P. 742–755.

[4] Farokhzad O.C., Langer R. Impact of Nanotechnology on Drug Delivery. *ACS Nano*, 2009, **3**(1), P. 16–20.

[5] Chen Y., Bose A., Bothun G.D. Controlled Release from Bilayer-Decorated Magnetoliposomes via Electromagnetic Heating. *ACS Nano*, 2010, **4**(6), P. 3215–3221.

[6] Ganta S., Devalapally H., Shahiwala A., Amiji M. A review of stimuli-responsive nanocarriers for drug and gene delivery. *J. Control Release*, 2008, **126**(3), P. 187–204.

[7] Torchilin V.P. *Nanoparticulates as drug carriers*. Imperial College Press, London, 2006, 754 p.

[8] Pal S.L., Jana U., Manna P.K., Mohanta G.P., Manavalan R. Nanoparticle: An overview of preparation and characterization. *J. Appl. Pharm. Sci.*, 2011, **1**(6), P. 228–234.

[9] Niu Z. Targeted transport therapeutic nanoparticles into adipose tissue. *J. Pharm. Drug Deliv. Res.*, 2018, **7**, P. 76.

[10] Alyautdin R., Khalin I., Nafeeza M.I., Haron M.H., Kuznetsov D. Nanoscale drug delivery systems and the blood–brain barrier. *Intern. J. Nanomed.*, 2014, **9**, P. 795–811.

[11] Lu C.T., Jin R.-R., Yi-Na Jiang Y.N., Lin Q., Yu W.-Z., Mao K.-L., Tian F.-R., Zhao Y.-P., Zhao Y-Z. Gelatin nanoparticle-mediated intranasal delivery of substance P protects against 6-hydroxydopamine-induced apoptosis: an *in vitro* and *vivo* study. *Drug Design, Development and Therapy*, 2015, **9**, P. 1955–1962.

[12] Sahoo S.K, Labhasetwar V. Enhanced antiproliferative activity of transferrin-conjugated paclitaxel-loaded nanoparticles is mediated via sustained intracellular drug retention. *Mol. Pharm.*, 2005, **2**, P. 373–383.

[13] Prabhu V., Uzzaman S., Grace V.M.B, Guruvayoorappan C. Nanoparticles in Drug Delivery and Cancer Therapy: The Giant Rats Tail. *J. Cancer Therapy*, 2011, **2**, P. 325–334.

[14] Gu F., Langer R., Omid C., Farokhzad O.C. Formulation/Preparation of Functionalized Nanoparticles for *In Vivo* Targeted Drug Delivery. *Micro and Nano Technologies in Bioanalysis, Methods in Molecular Biology (Humana Press, a part of Springer Science + Business Media, LLC 2009)*, 2009, **544**(Ch.37), P. 589–598.

[15] Jain K.K. The Role of Nanobiotechnology in Drug Discovery. *Drug Discover Today*, 2005, **10**(21), P. 1435–1442.

[16] Mishra B., Patel B.B., Tiwari S. Colloidal Nanocarriers: A Review on Formulation Technology, Types and Applications toward Targeted Drug Delivery, *Nanomed.*, 2010, **6**(1), P. 9–24.

[17] Majuru S., Oyewumi O. Nanotechnology in Drug Development and Life Cycle Management. *Nanotechnology in Drug Delivery*, 2009, **10**(4), P. 597–619.

[18] Pridgen E.M., Alexis F., Kuo T.T., Levy-Nissenbaum E., Karnik R., Blumberg R.S., Langer R., Farokhzad O.C Transepithelial Transport of Fc -Targeted Nanoparticles by the Neonatal Fc Receptor for Oral Delivery. *Sci. Transl. Med.*, 2013, **5**(213), P. 213–237.

[19] Yu M.K., Park J., Jon S. Targeting Strategies for Multifunctional Nanoparticles in Cancer Imaging and Therapy. *Theranostics*, 2012, **2**(1), P. 3–44.

[20] Allen T.M., Cullis P.R. Drug delivery systems: entering the mainstream. *Science*, 2004, **303**, P. 1818–1822.

[21] Brannon-Peppas L., Blanchette J.O. Nanoparticle and target systems for cancer therapy. *Adv. drug delivery rev.*, 2004, **56**, P. 1649–1659.

[22] Perr D., Karp J.M., Hong S., Farokhzad O.C., Magalit R., Langer R. Nanocarriers as an emerging platform for cancer therapy. *Nature nanotechnology*, 2007, **2**(12), P. 751–760.

[23] Lao J., Madani J., Puértolas T., Álvarez M., Hernández H., Pazo-Cid R.C., Artal A., Antonio A. Liposomal Doxorubicin in the Treatment of Breast Cancer Patients: A Review. *J. Drug Delivery*, 2013, **3**, P. 1–12.

[24] Bagherifam S., Skjeldal F.M., Griffiths G., Mælandsmo G.M., Olav Engebråten O, Nyström B., Hasirci V., Hasirci N. pH-Responsive Nano Carriers for Doxorubicin Delivery. *Pharm. Res.*, 2015, **32**, P. 1249–1263.

[25] Gardikis K., Tsimplouli C., Dimas K., Micha-Screttas M., Demetzos C. New chimeric advanced Drug Delivery nano Systems (chi-aDDnSs) as doxorubicin carriers. *Int. J. Pharm.*, 2010, **402**(1-2), P. 231–237.

[26] Hira S.K., Mishra A.K., Ray B., Manna P.P. Targeted Delivery of Doxorubicin-Loaded Poly(e-caprolactone)-b-Poly (N-vinylpyrrolidone) Micelles Enhances Antitumor Effect in Lymphoma. *PLoS ONE*, 2014, **9**(4), P. 1–17.
[27] Takahama H., Minamino T., Asanuma H. et al. Prolonged targeting of ischemic/reperfused myocardium by liposomal adenosine augments cardioprotection in rats. *J. Amer. College Cardiol.*, 2009, **53**(8), P. 709–717.
[28] Navarro G., Pan J., Torchilin V.P. Micelle-like Nanoparticles as Carriers for DNA and siRNA. *Mol. Pharm.*, 2015, **12**, P. 301–313.
[29] Zhang C., Zhu W., Liu Y., Yuan Z., Yang S., Chen W., Li J., Zhou X., Liu C., Zhang X. Novel polymer micelle mediated co-delivery of doxorubicin and P-glycoprotein siRNA for reversal of multidrug resistance and synergistic tumor therapy, 2016. (www.nature.com/scientificreports/). P. 1–12.
[30] Zuckerman J.E., Gritli I., Tolcher A., Heidel J.D., Lim D., Morgan R., Chmielowski B., Ribas A., Davis M.E., Yen Y. Correlating animal and human phase Ia/Ib clinical data with CALAA-01, a targeted, polymer-based nanoparticle containing siRNA. *Proc. Nat. Acad. Scie.*, 2014, **111**, P. 11449–11454.
[31] Baskar G., George G.B., Chamundeeswari M. Synthesis and Characterization of Asparaginase Bound Silver Nanocomposite Against Ovarian Cancer Cell Line A2780 and Lung Cancer Cell Line A549. *J. Inorg. and Organomet. Polymers and Mater.*, 2017, **27**(1), P. 87–94.
[32] Rosales-Martínez P., Cornejo-Mazón M., Arroyo-Maya I.J., Hernández-Sánchez H. Chitosan Micro- and Nanoparticles for Vitamin Encapsulation. *Nanotech. Appl. Food Industr.*, 2018, **19**, P. 429–442.
[33] Hwang J., Rodgers K., Oliver J.C., Schluep Th. α-Methylprednisolone conjugated cyclodextrin polymer-based nanoparticles for rheumatoid arthritis therapy. *Inter. J. Nanomed.*, 2008, **3**, P. 359–371.
[34] *Nanotechnology in Drug Delivery.* Ed. de Villiers M.M., Aramwit P., Kwon G.S.: Springer-Verlag, New York, 2009, 662 p.
[35] *Fundamentals and Applications of Controlled Release Drug Delivery.* Ed. Siepmann J., Siegel R.A., Rathbone M.J. Springer US, 2012, 594 p.
[36] Demetzos C. *Pharmaceutical Nanotechnology.* ADIS, 2016, 203 p.
[37] *Nanotechnology Applied To Pharmaceutical Technology.* Ed. Rai M., dos Santos C.A. Springer International Publishing, 2017, 386 p.
[38] Hoffman A.S. The origins and evolution of "controlled" drug delivery systems. *J. Controlled Release*, 2008, **132**(3), P. 153–163.
[39] Nanjunda Reddy B.H., Venkata Lakshmi V., Vishnu Mahesh K.R., Mylarappa M., Raghavendra N., Venkatesh T. Preparation of chitosan/different organomodified clay polymer nanocomposites: studies on morphological, swelling, thermal stability and antibacterial properties. *Nanosystems: Physics, Chemistry, Mathematics*, 2016, **7**(4), P. 667–674.
[40] Iwai K., Maeda H., Konno T. Use of oily contrast medium for selective drug targeting to tumor: enhanced therapeutic effect and X-ray image. *Cancer research*, 1984, **44**(5), P. 2115–2121.
[41] Kryuk T.V., Mikhal'chuk V.M., Petrenko L.V., Nelepova O.A., Nikolaevskii A.N. Antioxidative Stabilization of Polyethylene Glycol in Aqeous Solutions with Herb Phenols. *Russ. J. Appl. Chem.*, 2004, **77**(1), P. 131–135.
[42] Ostrovskii V.A. Interphase Transfer Catalysis of Organics Reactions. *Soros Education J.*, 2000. **6**(11), P. 30–34.
[43] Lasic D.D., Barenholz Y. *Handbook of nonmedical applications of liposomes: Theory and basic sciences*. **1**, CRC Press, Boca Raton, FL, USA, 1996, 368 p.
[44] Gobley T.N. Sur la lécithine et la cérébrine. *J. de Pharmacie et de Chimie*, 1874, **20**, P. 346–354.
[45] Strecker A. Ueber das Lecithin. *Annalen der Chemie und Pharmacie*, 1868, **148**(1), P. 77–90.
[46] Bangham A., Horne R. Negative staining of phospholipids and their structural modification by surface-active agents as observed in the electron microscope. *J. Molec. Biol.*, 1964, **8**(5), P. 660–668.
[47] Deshmukh R.R., Gawale S.V., Bhagwat M.K., Ahire P.A., Derle N.D. A review on liposomes. *World J. Pharm. Pharm. Sci.*, 2016, **5**(3), P. 506–517.
[48] Bangham A., Standish M., Watkins J. Diffusion of univalent ions across the lamellae of swollen phospholipids. *J. Molec. Biol.*, 1965, **13**(1), P. 238–252.
[49] Bozzuto G., Molinari A. Liposomes as nanomedical devices. *Int. J. Nanomed.*, 2015, **10**(1), P. 975–999.
[50] Biju S.S., Talegaonkar S., Mishra P.R., Khar R.K., Vesicular systems: An overview. *Ind. J. Pharm. Sci.*, 2006, **68**(2), P. 141–153.
[51] Garg T., K. Goyal A. Liposomes: Targeted and Controlled Delivery System. *Drug Delivery Lett.*, 2014, **4**(1), P. 62–71.
[52] Szoka F., Papahadjopoulos D. Procedure for preparation of liposomes with large internal aqueous space and high capture by reverse-phase evaporation. *Proc. Nat. Acad. Sci.*, 1978, **75**(9), P. 4194–4198.
[53] Akbarzadeh A., Rezaei-Sadabady R., Davaran S., Joo S.W., Zarghami N., Hanifehpour Y., Samiei M., Kouhi M., Nejati-Koshki K. Liposome: Classification, Preparation, and Applications. *Nanoscale Res. Lett.*, 2013, **8**(1), P. 102–110.
[54] Batzri S., Korn E.D. Single bilayer liposomes prepared without sonication. *Biochimica et Biophysica Acta (BBA)-Biomembranes*, 1973, **298**(4), P. 1015–1019.
[55] Olson F., Hunt C.A., Szoka F.C., Vail W.J., Papahadjopoulos D. Preparation of liposomes of defined size distribution by extrusion through polycarbonate membranes. *Biochimica et Biophysica Acta (BBA)-Biomembranes*, 1979, **557**(1), P. 9–23.
[56] Touitou E., Junginger H., Weiner N., Nagai T., Mezei M. Liposomes as Carriers for Topical and Transdermal Delivery. *J. Pharm. Sci.*, 1994, **83**(9), P. 1189–1203.
[57] Touitou E., Levi-Schaffer F., Dayan N., Alhaique F., Riccieri F. Modulation of Caffeine Skin Delivery by Carrier Design: Liposomes versus Permeation Enhancers. *Int. J. Pharm.*, 1994, **103**(2), P. 131–136.
[58] Laouini A., Jaafar-Maalej C., Limayem-Blouza I., Sfar S., Charcosset C., Fessi H. Preparation, Characterization and Applications of Liposomes: State of the Art. *J. Colloid Sci. and Biotechn.*, 2012, **1**(2), P. 147–168.
[59] Torchilin V.P. Recent advances with liposomes as pharmaceutical carriers. *Nat. Rev. Drug Discov.*, 2005, **4**, P. 145–160.
[60] Takahama H., Minamino T., Asanuma H. Fujita M., Asai T., Wakeno M., Sasaki H., Kikuchi H., Hashimoto K., Oku N., Asakura M., Kim J., Takashima S., Komamura K., Sugimachi M., Mochizuki N., Kitakaze M. Prolonged targeting of ischemic/reperfused myocardium by liposomal adenosine augments cardioprotection in rats. *J. Amer. College of Cardiology*, 2009, **53**(8), P. 709–717.
[61] Gregoriadis G., Swain C.P., Wills E.J., Tavill A.S. Drug-carrier potential of liposomes in cancer chemotherapy. *Lancet,* 1974, **1**, P. 1313–1316.
[62] Tam Y.C., Chen S., Cullis P.R. Advances in Lipid Nanoparticles for siRNA Delivery, *Pharmaceutic*, 2013, **5**, P. 498–507.
[63] Anwekar H., Patel S., Singhai A.K. Liposomes as drug carriers. *Int. J. Pharm. Life Sci.* (IJPLS), 2011, **2**(7), P. 945–951.
[64] Akbarzadeh A., Rezaei-Sadabady R., Nejati K. Liposome: classification, preparation, and applications. *Nanoscale Research Letters*, 2013, **8**(1), P. 102–111.

[65] Johnston M.J., Semple S.C., Klimuk S.K., Ansell S., Maurer N., Cullis P.R. Characterization of the drug retention and pharmacokinetic properties of liposomal nanoparticles containing dihydrosphingomyelin. *Biochim. Biophys. Acta*, 2007, **1768**, P. 1121–1127.
[66] Raney S.G., Wilson K.D., Sekirov L., Chikh G., de Jong S.D., Cullis P.R., Tam Y.K. The effect of circulation lifetime and drug-to-lipid ratio of intravenously administered lipid nanoparticles on the biodistribution and immunostimulatory activity of encapsulated CpG-ODN. *J. Drug. Target*, 2008, **16**(7), P. 564–77.
[67] Fenske D.B., Chonn A. Cullis. Liposomal Nanomedicines: An Emerging Field. *Toxicologic Pathology*, 2008, **36**, P. 21–29.
[68] Fenske D.B., Cullis P.R. Liposomal Nanomedicines. *Expert Opin. Drug. Deliv.*, 2008, **5**(1), P. 25–44.
[69] Barsukov L.I. Liposomes. *Soros Education J.*, 1998, **10**, P. 2–9.
[70] Smyslov R.Yu., Ezdakova K.V., Kopitsa G.P., Khripunov A.K., Bugrov A.N., Tkachenko A.A., Angelov B., Pipich V., Szekely N.K., Baranchikov A.E., Latysheva E., Chetverikov Yu.O., Haramus V. Morphological structure of *Gluconacetobacter xylinus* cellulose and cellulose-based organic-inorganic composite materials. *J. Phys.: Conf. Ser.*, 2017, **848**(1), P. 012017.
[71] Almjasheva O.V., Garabadzhiu A.V., Kozina Yu.V., Litvinchuk L.F., Dobritsa V.P. Biological effect of zirconium dioxide-based nanoparticles. *Nanosystems: Physics, Chemistry, Mathematics*, 2017, **8**(3), P. 391–396.
[72] Bugrov A.N., Zavialova A.Yu., Smyslov R.Yu., Anan'eva T.D., Vlasova E.N., Mokeev M.V., Kryukov A.E., Kopitsa G.P., Pipich V. Luminescence of Eu^{3+} ions in hybrid polymer-inorganic composites based on poly(methyl methacrylate) and zirconia nanoparticles. *Luminescence*, 2018, **33**(5), P. 837–849.
[73] Popov A.L., Shcherbakov A.B., Zholobak N.M., Baranchikov A.Ye., Ivanov V.K. Cerium dioxide nanoparticles as third-generation enzymes (nanozymes). *Nanosystems: Physics, Chemistry, Mathematics*, 2017, **8**(6), P. 760–781.
[74] Bugrov A.N., Rodionov I.A., Zvereva I.A., Smyslov R.Yu., Almjasheva O.V. Photocatalytic activity and luminescent properties of Y, Eu, Tb, Sm and Er-doped ZrO_2 nanoparticles obtained by hydrothermal method. *Int. J. Nanotechnology*, 2016, **13**(1/2/3), P. 147–157.
[75] Shydlovska O., Kharchenko E., Zholobak N., Shcherbakov A., Marynin A., Ivanova O., Baranchikov A., Ivanov V. Cerium oxide nanoparticles increase the cytotoxicity of TNF alpha *in vitro*. *Nanosystems: Physics, Chemistry, Mathematics*, 2018, **9**(4), P. 537–543.
[76] Almjasheva O.V., Smirnov A.V., Fedorov B.A., Tomkovich M.V., Gusarov V.V. Structural features of ZrO_2-Y_2O_3 and ZrO_2-Gd_2O_3 nanoparticles formed under hydrothermal conditions. *Russ. J. Gen. Chem.*, 2014, **84**(5), P. 804–809.
[77] Popov A.L., Savintseva I.V., Mysina E.A., Shcherbakov A.B., Popova N.R., Ivanova O.S., Kolmanovich D.D., Ivanov V.K. Cytotoxicity analysis of gadolinium doped cerium oxide nanoparticles on human mesenchymal stem cells. *Nanosystems: Physics, Chemistry, Mathematics*, 2018, **9**(3), P. 430–438.
[78] Jayakumar G., Irudayaraj A., Dhayal Raj A., Anusuya M. Investigation on the preparation and properties of nanostructured cerium oxide. *Nanosystems: Physics, Chemistry, Mathematics*, 2016, **7**(4), P. 728–731.
[79] Vardanyan Z., Gevorkyan V., Ananyan M., Vardapetyan H., Trchounian A. Effects of various heavy metal nanoparticles on *Enterococcus hirae* and *Escherichia coli* growth and proton-coupled membrane transport. *J. Nanobiotechnol*, 2015, **13**(69), P. 2–9.
[80] Bugrov A.N., Smyslov R.Yu., Zavialova A.Yu., Kirilenko D.A., Pankin D.V. Phase composition and photoluminescence correlations in nanocrystalline ZrO_2:Eu^{3+} phosphors synthesized under hydrothermal conditions. *Nanosystems: Physics, Chemistry, Mathematics*, 2018, **9**(3), P. 378–388.
[81] Popov A.L., Ermakov A.M., Shekunova T.O., Shcherbakov A.B., Ermakova O.N., Ivanova O.S., Popova N.R., Baranchikov A.Ye., Ivanov V.K. PVP-stabilized tungsten oxide nanoparticles inhibit proliferation of NCTC L929 mouse fibroblasts via induction of intracellular oxidative stress. *Nanosystems: Physics, Chemistry, Mathematics*, 2019, **10**(1), P. 92–101.
[82] Sharker S.Md., Kim S.M., Lee J.E., Choi K.H., Shin G., Lee S., Lee D.K., Jeong J., Park S.Y. Functionalized biocompatible WO_3 nanoparticles for triggered and targeted *in vitro* and *in vivo* photothermal therapy. *J. Control. Release*, 2015, **217**, P. 211–220.
[83] Zhou Z., Kong B., Yu C., Shi X., Wang M., Liu W., Sun Y., Zhang Y., Yang H., Yang S. Tungsten Oxide Nanorods: An Efficient Nanoplatform for Tumor CT Imaging and Photothermal Therapy. *Sci. Rep.*, 2014, **4**, P. 3653–3663.
[84] Xing Y., Li L., Ai X., Fu L. Polyaniline-coated upconversion nanoparticles with upconverting luminescent and photothermal conversion properties for photothermal cancer therapy. *Intern. J. Nanomed.*, 2016, **11**, P. 4327–4338.
[85] Popov A.L., Savintseva I.V., Mysina E.A., Shcherbakov A.B., Popova N.R., Ivanova O.S., Kolmanovich D.D., Ivanov V.K. Cytotoxicity analysis of gadolinium doped cerium oxide nanoparticles on human mesenchymal stem cells. *Nanosystems: Physics, Chemistry, Mathematics*, 2018, **9**(3), P. 430–438.
[86] Slowing I.I. Mesoporous silica nanoparticles as controlled release drug delivery and gene transfection carriers. *Adv. Drug Deliv. Rev.*, 2008, **60**(11), P. 1278–1288.
[87] Vasilevskaya A. K., Almjasheva O.V., Gusarov V.V. Formation of nanocrystals in the ZrO_2–H_2O system. *Russ. J. Gen. Chem.*, 2015, **85**(12), P. 1937–1942.
[88] Popkov V.I., Tugova E.A., Bachina A.K., Almyasheva O.V. The formation of nanocrystalline orthoferrites of rare-earth elements $XFeO_3$ (X = Y, La, Gd) via heat treatment of coprecipitated hydroxides. *Russ. J. Gen. Chem.*, 2017, **87**(11), P. 1771–1780.
[89] Popkov V.I., Almjasheva O.V., Semenova A.S., Kellerman D.G., Nevedomskiy V.N., Gusarov V.V. Magnetic properties of $YFeO_3$ nanocrystals obtained by different soft-chemical methods. *J. Mater Sci: Mater Electron.*, 2017, **28**(10), P. 7163–7170.
[90] Berezhnaya M.V., Al'myasheva O.V., Mittova V.O., Nguen A.T., Mittova I.Ya. Sol-Gel Synthesis and Properties of $Y_{1-x}Ba_xFeO_3$ Nanocrystals. *Russ. J. Gen. Chem.*, 2018, **88**(4), P. 626–631.
[91] Komlev A.A., Panchuk V.V., Semenov V.G., Almjasheva O.V., Gusarov V.V. Effect of the sequence of chemical transformations on the spatial segregation of components and formation of periclase-spinel nanopowders in the MgO–Fe_2O_3–H_2O System. *Russ. J. Appl. Chem.*, 2016, **89**(12), P. 1932–1938.
[92] Kuznetsova V.A., Almjasheva O.V., Gusarov V.V. Influence of microwave and ultrasonic treatment on the formation of $CoFe_2O_4$ under hydrothermal conditions. *Glass Phys. Chem.*, 2009, **35**(2), P. 205–209.
[93] Proskurina O.V., Tomkovich M.V., Bachina A.K., Sokolov V.V., Danilovich D.P., Panchuk V.V., Semenov V.G., Gusarov V.V. Formation of Nanocrystalline $BiFeO_3$ under Hydrothermal Conditions. *Russ. J. Gen. Chem.*, 2017, **87**(11), P. 2507–2515.
[94] Almjasheva O.V., Gusarov V.V. Prenucleation formations in control over synthesis of $CoFe_2O_4$ nanocrystalline powders. *Russ. J. Appl. Chem.*, 2016, **89**(6), P. 689–695.
[95] Sharikov F.Yu., Almjasheva O.V., Gusarov V.V. Thermal analysis of formation of ZrO_2 nanoparticles under hydrothermal conditions. *Russ. J. Inorg. Chem.*, **51**(10), P. 1538–1542.

[96] Almjasheva O.V., Gusarov V.V. Prenucleation formations in control over synthesis of $CoFe_2O_4$ nanocrystalline powders. *Russ. J. Appl. Chem.*, 2016, **89**(6), P. 851–856.
[97] Almjasheva O.V., Krasilin A.A., Gusarov V.V. Formation mechanism of core-shell nanocrystals obtained via dehydration of coprecipitated hydroxides at hydrothermal conditions. *Nanosystems: Phys. Chem. Math.*, 2018, **9**(4), P. 568–572.
[98] Abiev R.Sh., Al'myasheva O.V., Gusarov V.V., Izotova S.G. Method of producing nanopowder of cobalt ferrite and microreactor to this end. RF Patent 2625981, Bull. **20**, 20.07.2017.
[99] Abiev R.S., Almyasheva O.V., Izotova S.G., Gusarov V.V. Synthesis of cobalt ferrite nanoparticles by means of confined impinging-jets reactors. *J. Chem. Tech. App.*, 2017, **1**(1), P. 7–13.
[100] Proskurina O.V., Nogovitsin I.V., Il'ina T.S., Danilovich D.P., Abiev R.Sh., Gusarov V.V. Formation of $BiFeO_3$ Nanoparticles Using Impinging Jets. *Microreactor. Russ. J. Gen. Chem.*, 2018, **88**(10), P. 2139–2143.
[101] Bugrov A.N., Vlasova E.N., Mokeev M.V., Popova E.N., Ivan'kova E.M., Al'myasheva O.V., Svetlichnyi V.M. Distribution of zirconia nanoparticles in the matrix of poly(4,4′-oxydiphenylenepyromellitimide). *Polym. Sci. Ser. B.*, 2012, **54**(9-10), P. 486–495.
[102] Almjashev O.V., Gusarov V.V. Effect of ZrO_2 nanocrystals on the stabilization of the amorphous state of alumina and silica in the ZrO_2-$Al_2O_3$and ZrO_2-SiO_2 systems. *Glass Phys. Chem.*, 2006, **32** (2), P. 162–166.
[103] Kotov Y.A. Electric explosion of wires as a method for preparation of nanopowders. *J. Nanoparticle Research*, 2003, **5**(5-6), P. 539–550.
[104] Kotov Y.A., Azarkevich E.I., Beketov I.V., Demina T.M., Murzakaev A.M., Samatov O.M. Producing A1 and A1203 nanopowders by electrical explosion of wire. *Key Engineering Materials*, 1997, **132–136**, P. 173–176.
[105] Kotov Y.A., Samatov O.M. Production of nanometer-sized A1N powders by the exploding wire method. *Nanostruct. Mater.*, 1999, **12**, P. 119–122.
[106] Sherman P. Generation of submicron metal particles. *Colloid and Interface Sci.*, 1975, **51**(1), P. 87–93.
[107] Karioris F., Fish B. An Exploding Wire Aerosol Generator. *J. Colloid Science*, 1962, **17**, P. 155–161.
[108] Bennett F.D. High-temperature cores in exploding wires. *Phys. Fluids*, 1965, **8**(6), P. 1106–1108.
[109] Chace W.G. Exploding Wires. Phisics Today, 1964, **17**(87), P. 19.
[110] Kaori K., Hirashi I., Vasio M. The formation and characteristics of Powders by wire explosion. 2-nd report. *Nippon Tungsten Rev.*, 1972, **5**, P. 20.
[111] Gusev A.I., Rempel A.A. *Nanocrystalline Materials*. Cambridge, International Science Publishing Cambridge, 2004, 351 p.
[112] Alymov M.I., Maltina E.I., Stepanov Y.N. Model of Initial Stage of Ultrafme Metal Powder Sintering. *Nanostructured Mater.*, 1994, **4**(6), P. 737–742.
[113] Bennett F.D., Kahl G.D., Wedemeyer E.H. Resistance Changes caused by Vaporization Waves Exploding Wires. *Exploding Wires*, 1964, **3**, Plenum Press, New York, 1964, P. 65–84.
[114] Ivanov G., Lerner M., Tepper F. Intermetallic Alloy Formation from Nanophase Metal Powders Produced by Electro-Exploding Wires. *Advances in Powder Metallurgy & Particulate Materials*, 1996, **40**, P. 15/55–15/63.
[115] Jonson R., Siegel B. Chemical Reactor Utilising Successive Multiple Electrical Explosions of Metal Wires. *Rev. Sci. Instr.*, 1970, **42**(6), P. 854–859.
[116] Miller J.C. A brief history of laser ablation. Laser ablation: mechanisms and applications – II. *AIP Publishing*, 1993, **2889**(1), P. 619–622.
[117] Kirichenko N.A., Sukhov I.A., Shafeev G.A., Shcherbina M.E. Evolution of the distribution function of Au nanoparticles in a liquid under the action of laser radiation. *Quantum Electronics*, 2012, **42**(2), P. 175–180.
[118] Sukhov I.A., Shafeev G., Voronov V.V., Sygletou M., Stratakis E., Fotakis C. Generation of nanoparticles of bronze and brass by laser ablation in liquid. *Appl. Surface Sci.*, 2014, **302**, P. 79–82.
[119] Zhil'nikova M.I., Barmina E.V., Shafeev G.A. Laser-Assisted Formation of Elongated Au Nanoparticles and Subsequent Dynamics of Their Morphology under Pulsed Irradiation in Water. *Physics of Wave Phenomena*, 2018, **26**(2), P. 85–92.
[120] Hiramatsu H., Osterloh F.E. A simple large-scale synthesis of nearly monodisperse gold and silver nanoparticles with adjustable sizes and with exchangeable surfactants. *Chem. Mater.*, 2004, **16**(13), P. 2509–2511.
[121] Simakin A.V., Voronov V.V., Shafeev G.A., Brayner R. Nanodisks of Au and Ag produced by laser ablation in liquid environment. *Chem. Phys. Lett.*, 2001, **348**(3), P. 182–186.
[122] Kuzmin P.G., Shafeev G.A., Viau G., Warot-Fonrose B., Barberoglou M., Stratakis E., Fotakis C. Porous nanoparticles of Al and Ti generated by laser ablation in liquids. *Appl. Surf. Sci.*, 2012, **258**(23), P. 9283–9287.
[123] Amendola V., Riello P., Meneghetti M., 2011. Magnetic Nanoparticles of Iron Carbide, Iron Oxide, Iron@Iron Oxide, and Metal Iron Synthesized by Laser Ablation in Organic Solvents. *J. Phys. Chem. C*, 2010, **115**(12), P. 5140–5146.
[124] Tsuji T., Iryo K., Watanabe N., Tsuji M. Preparation of silver nanoparticles by laser ablation in solution: influence of laser wavelength on particle size. *Appl. Surf. Sci.*, 2002, **202**(1–2), P. 80–85.
[125] Dolgaev I., Simakin A.V., Voronov V.V., Shafeev G.A., Bozon-Verduraz F. Nanoparticles produced by laser ablation of solids in liquid environment. *Appl. Surf. Sci.*, 2002, **186**(1), P. 546–551.
[126] Kamat P.V., Flumiani M., Hartland G.V. Picosecond dynamics of silver nanoclusters. Photoejection of electrons and fragmentation. *J. Phys. Chem. B.*, 1998, **102**(17), P. 3123–3128.
[127] Hamad A., Li L., Liu Z. A comparison of the characteristics of nanosecond, picosecond and femtosecond lasers generated Ag, TiO_2 and Au nanoparticles in deionised water. *Appl. Phys. A*, 2015, **120**(4), P. 1247–1260.
[128] Kurland H.-D., Stotzel Ch., Grabow J., Zink I., Müller E., Staupendahl G., Müller F.A. Preparation of Spherical Titania Nanoparticles by CO_2 Laser Evaporation and Process-Integrated Particle Coating. *J. Amer. Ceram. Soc.*, 2010, **93**(5), P. 1282–1289.
[129] Popp U., Herbig R., Michel G., Müller E., Oestreich Ch. Properties of nanocrystalline ceramic powders prepared by laser evaporation and recondensation. *J. Eur. Ceram. Soc.*, 1998, **18**, P. 1153–116.
[130] Osipov V.V., Kotov Yu.A., Ivanov M.G., Samatov O.M., Lisenkov V.V., Platonov V.V., Murzakayev A.M., Medvedev A.I., Azarkevich E.I. Laser synthesis of nanopowders. *Laser Phys.*, 2006, **16**(1), P. 116–125.
[131] Kurland H.D., Grabow J., Staupendahl G., Andre M.E., Dutz S., Bellemann M.E. Magnetic iron oxide nanopowders produced by CO_2 laser evaporation. *J. Magnet., Magn. Mater.*, 2007, **311**, P. 73–77.
[132] Sato T., Diono W., Sasaki M., Goto M. Silver nanoparticles generated by pulsed laser ablation in supercritical CO_2 medium. *High Pressure Res.*, 2012, **32**(1), P. 1–7.

[133] Varma A., Mukasyan A.S., Deshpande K.T., Pranda P., Erri P.R. Combustion Synthesis of Nanoscale Oxide Powders: Mechanism, Characterization and Properties. *MRS Proc.*, 2003, **800**, P. AA4.1–AA4.12.
[134] Mokkelbost T., Kaus I., Grande T., Einarsrud M.A. Combustion Synthesis and Characterization of Nanocrystalline CeO_2 Based Powders. *Chem. Mater.*, 2004, **16**(25), P. 5489–5494.
[135] Wang X., Qin M., Fang F., Jia B., Wu H., Qu X., Volinsky A.A. Effect of glycine on onestep solution combustion synthesis of magnetite nanoparticles. *J. Alloys Compd.*, 2017, **719**, P. 288–295.
[136] Mukasyan A.S., Epstein P., Dinka P. Solution combustion synthesis of nanomaterials. *Proc. Combust. Inst.*, 2007, **31**(2), P. 1789–1795.
[137] Rogachev A.S., Mukasyan A.S. *Combustion for Material Synthesis*. Boca Raton, CRC Press, 2014, 424 p.
[138] Varma A., Mukasyan A.S., Rogachev A.S., Manukyan K.V. Solution Combustion Synthesis of Nanoscale Materials. *Chem. Rev.*, 2016, **116**(23), P. 14493–14586.
[139] Ostroushko A.A. Russkikh O.V. Oxide Material Synthesis by Combustion of Organic-Inorganic Compositions. *Nanosystems: Physics, Chemistry, Mathematics*, 2017, **8**(4), P. 476–502.
[140] Kuchma E., Zolotukhin P., Belanova A., Soldatov M., Lastovina T., Kubrin S., Nikolsky A., Mirmikova L., Soldatov A. Low Toxic Maghemite Nanoparticles for Theranostic Applications. *International Journal of Nanomedicine*, 2017, **12**, P. 6365–6371.
[141] Lojk J., Bregar V.B., Strojan K., Hudoklin S., Verani P., Pavlin M., Kreft M.E. Increased Endocytosis of Magnetic Nanoparticles into Cancerous Urothelial Cells versus Normal Urothelial Cells. *Histochemistry and Cell Biology*, 2018, **149**(1), P. 45–59.
[142] Firouzi M., Poursalehi R., Delavari H., Saba F., Oghabian M.A. Chitosan coated tungsten trioxide nanoparticles as a contrast agent for X-ray computed tomography. *Int. J. Biol. Macromol.*, 2017, **98**, P. 479–485.
[143] Gelperina S., Maksimenko O., Khalansky A., Vanchugova L., Shipulo E., Abbasova K., Berdiev R., Wohlfart S., Chepurnova N., Kreuter J. Drug delivery to the brain using surfactant-coated poly (lactideco-glycolide) nanoparticles: influence of the formulation parameters. *Eur. J. Pharm. Biopharm.*, 2010, **74**, P. 157–163.
[144] Popova N.R., Popov A.L., Shcherbakov A.B., Ivanov V.K. Layer-by-layer capsules as smart delivery systems of CeO_2 nanoparticle-basedtheranostic agents. *Nanosystems: Physics, Chemistry, Mathematics*, 2017, **8**(2), P. 282–289.
[145] Venkatesan H., Radhakrishnan S., Parthibavarman M., Kumar R.D., Sekar C. Synthesis of polyethylene glycol (PEG) assisted tungsten oxide (WO_3) nanoparticles for L-dopa bio-sensing applications. *Talanta*, 2011, **85**(4), P. 2166–2174.
[146] Porcel E., Liehn S., Remita H., Usami N., Kobayashi K., Furusawa Y., Sech C.L., Lacombe S. Platinum Nanoparticles: A Promising Material for Future Cancer Therapy? *Nanotechnology*, 2010, **21**(8), P. 85–103.
[147] Mornet S., Vasseur S., Grasset F., Duguet E. Magnetic Nanoparticle Design for Medical Diagnosis and Therapy. *Journal of Materials Chemistry*, 2004, **14**(14), P. 2161–2175.
[148] Garanina A.S., Kireev I.I., Alieva I.B., Majouga A.G., Davydov V.A., Murugesan S., Khabashesku V.N., Agafonov V.N., Uzbekov R.E. New superparamagnetic fluorescent Fe@C-$C_5ON_2H_{10}$-Alexa Fluor 647 nanoparticles for biological applications. *Nanosystems: Physics, Chemistry, Mathematics*, 2018, **9**(1), P. 120–122.
[149] Morones J.R., Elechiguerra J.L., Camacho A., Holt K, Kouri J.B., Ramirez J.T., Yacaman M.J. The Bactericidal Effect of Silver Nanoparticles. *Nanotechnology*, 2005, **16**(10), P. 2346–2353.
[150] Alieva I., Kireev I., Rakhmanina A., Garanina A., Strelkova O., Zhironkina O., Cherepaninets V., Davydov V., Khabashesku V., Agafonov V., Uzbekov R. Magnetinduced behavior of iron carbide (Fe_7C_3@C) nanoparticles in the cytoplasm of living cells. *Nanosystems: Physics, Chemistry, Mathematics*, 2016, **7**(1), P. 158–160.
[151] Koulikova M., Kochubey V.I. Synthesis and Optical Properties of Iron Oxide Nanoparticles for Photodynamic Therapy. *Reports of Samara Scientific Center of Russian Academy of Sciences (RAS)*, 2012, **14**(4), P. 206–209.
[152] Selvamuthumari J., Meenakshi S., Ganesan M., Nagaraj S., Pandian K. Antibacterial and catalytic properties of silver nanoparticles loaded zeolite: green method for synthesis of silver nanoparticles using lemon juice as reducing agent. *Nanosystems: Physics, Chemistry, Mathematics*, 2016, **7**(4), P. 768–773.
[153] Dykman L.A., Khlebtsov N.G. Gold Nanoparticles in Biology and Medicine: Recent Advances and Prospects. *Acta Naturae*, 2011, **3**(2), P. 34–55.
[154] Preethika R.K., Ramya R., Ganesan M., Nagaraj S., Pandian K. Synthesis and characterization of neomycin functionalized chitosan stabilized silver nanoparticles and study its antimicrobial activity. *Nanosystems: Physics, Chemistry, Mathematics*, 2016, **7**(4), P. 759–764.
[155] Akbarzadeh A., Mohammad Samiei M., Soodabeh Davaran S. Magnetic nanoparticles: preparation, physical properties, and applications in biomedicine. *Nanoscale Res. Lett.*, 2012, **7**, P. 144–157.
[156] Tartaj P., Morales M.D.D., Veintemillas-Verdaguer S., Gonzalez-Carreno T., Serna C.J. The preparation of magnetic nanoparticles for applications in biomedicine. *J. Phys. D: Appl. Phys.*, 2003, **36**, P. R182–R197.
[157] Ghadiri M., Vasheghani-Farahani E., Atyabi F., Kobarfard F., Mohamadyar-Toupkanlou F., Hosseinkhani H. Transferrin-conjugated magnetic dextran-spermine nanoparticles for targeted drug transport across blood-brain barrier. *J. Biomed. Mater. Res. A*, 2017, **105A**(10), P. 2851–2864.
[158] MacBain S.C., Yiu H.H., Dobson J. Magnetic nanoparticles for gene and drug delivery *Int. J. Nanomed.*, 2008, **3**(2), P. 169–180.
[159] Akbarzadeh A., Asgari D., Zarghami N., Mohammad R., Davaran S. Preparation and in vitro evaluation of doxorubicin-loaded Fe_3O_4 magnetic nanoparticles modified with biocompatible co-polymers. *Int. J. Nanomed.*, 2012, **7**, P. 511–526.
[160] Akbarzadeh A., Zarghami N., Mikaeili H., Asgari D., Goganian A.M., Khiabani H.K., Samiei M., Davaran S. Synthesis, characterization, and in vitro evaluation of novel polymer-coated magnetic nanoparticles for controlled delivery of doxorubicin. *Nanotechnol. Sci. Appl.*, 2012, **5**, P. 13–25.
[161] Reddy L.H., Arias J.L., Nicolas J., Couvreur P. Magnetic nanoparticles: design and characterization, toxicity and biocompatibility, pharmaceutical and biomedical applications. *Chem. Rev.*, 2012, **112**, P. 5818–5878.
[162] Kayal S., Ramanujan R.V. Anti-cancer drug loaded iron – gold core – shell nanoparticles (Fe@Au) for magnetic drug targeting. *J. Nanosci. Nanotechnol.*, 2010, **10**, P. 5527–5539.
[163] Sharker S.M., Kim S.M., Lee J.E., Choi K.H., Shin G., Lee S., Lee K.G., Jeong J., Lee H., Park S.Y. Functionalized biocompatible WO_3 nanoparticles for triggered and targeted in vitro and in vivo photothermal therapy. *J. Control. Release*, 2015, **217**, P. 211–220.
[164] Popov A., Zholobak N., Balko O.I., Balko O.B., Shcherbakov A.B., Popova N.R., Ivanova-Polezhaeva O.S., Baranchikov A.E., Ivanov V.K. Photo-induced toxicity of tungsten oxide photochromic nanoparticles. *J. Photochem. Photobiol. B*, 2018, **178**, P. 395–403.

[165] Qiu J., Xiao Q., Zheng X., Zhang L., Xing H., Ni D., Liu Y., Zhang S., Ren Q., Hua Y., Zhao K., Bu W. Single $W_{18}O_{49}$ nanowires: A multifunctional nanoplatform for computed tomography imaging and photothermal/photodynamic/radiation synergistic cancer therapy. *Nano Research*, 2015, **8**(11), P. 3580–3590.

[166] Li G., Chen Y., Zhang L., Zhang M., Li S.,.Li L., Wang T., Wang C. Nano-Micro Lett. Facile Approach to Synthesize Gold Nanorod@Polyacrylic Acid/Calcium Phosphate Yolk–Shell Nanoparticles for Dual-ModeImaging and pH/NIR-Responsive Drug Delivery. *Nano-Micro Lett.*, 2018, **10**(7), P. 1–11.

[167] Espinosa A., Corato R.D., Kolosnjaj-Tabi J., Flaud P., Pellegrino T., Wilhelm C. Duality of Iron Oxide Nanoparticles in Cancer Therapy: Amplification of Heating Efficiency by Magnetic Hyperthermia and Photothermal Bimodal Treatment. *ACS Nano*, 2016, **10**(2), P. 2436–2446.

[168] Antonii F. *Panacea aurea-auro potabile*. Hamburg, Ex Bibliopolio Frobeniano, 1618, 238 p.

[169] Guterres S.S., Poletto F., Colom'e L., Raffin R., Pohlmann A. Polymeric Nanocapsules for Drug Delivery: An Overview. *Colloids in Drug Delivery*, 2010, Taylor & Francis/CRC Press, **3**, P. 71–98.

[170] Yiyun C., Zhenhua X., Minglu M., Tonguen X. Dendrimers as Drug Carriers: Applications in Different Routes of Drug. *J. Pharma. Sci.*, 2008, **97**(1), P. 123–143.

[171] Inagamov S.Y., Sattarov S.S., Shadmanov K.K., Karimov A.K. Interpolymer complexes on the basis of sodium carboxymethyl cellulose – carriers nanoparticles of medicinal preparations. Mat. Conf. (Munich, Germany, 31 Oct. – 5 Nov. 2018). Education and science without borders, Fundamental and applied research in nanotechnology, 2018, **6**, (http://www.science-sd.com/478-25428 and http://www.science-sd.com/pdf/2018/6/25428.pdf).

[172] Lu C.T., Jin R.R., Jiang Y.N., Lin Q., Yu W.Z., Mao K.L., Tian F.R., Zhao Y.P., Zhao Y.Z. Gelatin nanoparticle-mediated intranasal delivery of substance P protects against 6-hydroxydopamine-induced apoptosis: an in vitro and in vivo study. *Drug Design, Development and Therapy*, 2015, **9**, P. 1955–1962.

[173] Svenson S. Dendrimers as versatile platform in drug delivery applications. *Eur. J. Pharm. Biopharm*, 2009, **71**, P. 445–462.

[174] Chan J.M., Valencia P.M., Zhang L., Langer R., Farokhzad O.C. Polymeric Nanoparticles for Drug Delivery. *Cancer Nanotechnology*, 2010, **624**, P. 163–175.

[175] Sambanis A. Encapsulated cell systems: the future of insulin delivery? *Therapeutic delivery*, 2012, **3**, P. 1029–1032.

[176] Zhang Y., Chan H.F., Leong K.W. Advanced materials and processing for drug delivery: the past and the future. *Adv. Drug Delivery Rev.*, 2013, **65**, P. 104-120.

[177] Hernández R.M., Orive G., Murua A., Pedraz J.L. Microcapsules and microcarriers for in situ cell delivery. *Adv. Drug Delivery Rev.*, 2010, **62**, P. 711–730.

[178] De Geest B.G., De Koker S., Sukhorukov G.B., Kreft O., Parak W.J., Skirtach A.G., Demeester J., De Smedt S.C., Hennink W.E. Polyelectrolyte microcapsules for biomedical applications. *Soft Matter.*, 2009, **5**, P. 282–291.

[179] Jämsä S., Mahlberg R., Holopainen U., Ropponen J., Savolainen A., Ritschkoff A.-C. Slow release of a biocidal agent from polymeric microcapsules for preventing biodeterioration. *Progress in Organic Coatings*, 2013, **76**, P. 269–276.

[180] Kaur I.P., Singh H. Nanostructured drug delivery for better management of tuberculosis. *J. Controlled Release*, 2014, **184**, P. 36–50.

[181] Hamley I.W., Castelletto V., Fundin J., Crothers M., Attwoodand D., Talmon Y. Close-packing of Diblock Copolymer Micelles. *Colloid Polym. Sci.*, 2004, **282**, P. 514–517.

[182] Hamley I.W. Nanoshells and Nanotubes from Block Copolymers. *Soft Matter.*, 2005, **1**, P. 36–43.

[183] Taboada P., Velasquez G., Barbosa S., Castelletto V., Nixon S.K., Yang Z., Heatley F., Hamley I.W., Mosquera V., Ashford M., Attwoodand D., Booth C. Block copolymers of ethylene oxide and phenyl glycidyl ether: Micellization, gelation and drug solubilization. *Langmuir*, 2005, **21**, P. 5263–5271.

[184] Manjappa A.S., Chaudhari K.R., Venkataraju M.P., Dantuluri P., Nanda B., Sidda C., Sawant K.K., Murthy R.S.R. Antibody derivatization. *J. Controlled Release*, 2011, **150**(1), P. 2–22.

[185] Kedar U., Phutane P., Shidhaye S., Kadam V. Advances in polymeric micelles for drug delivery and tumor targeting. *Nanomed.*, 2010, **6**, P. 714–729.

[186] Wagh A., Law B. Methods for Conjugating Antibodies to Nanocarriers. In: Ducry L. (eds.) Antibody-Drug Conjugates. *Methods in Molecular Biology (Methods and Protocols)*, 2013, **1045**, P. 249–266.

[187] Cui J., Fan D., Hao J. Magnetic $Mo_{72}Fe_{30}$-embedded hybrid nanocapsules. *Journal of colloid and interface science*, 2009, **330**(2), P. 488–492.

[188] Kroto H.W., Heath J.R., O'Brien S.C., Curl, R.F. C_{60}: Buckminsterfullerene. *Nature*, 1985, **318**, P. 162–163.

[189] Kratschmer W., Lamb L.D., Fostiropoulos K., Huffman D.R. Solid C_{60}: a new form of carbon. *Nature*, 1990, **347**(6291), P. 354–358.

[190] Ala'a K. Isolation, separation and characterisation of the fullerenes C_{60} and C_{70}: the third form of carbon. *J. Chemical Soc., Chem. Commun.*, 1990, **20**, P. 1423–1425.

[191] Gerasimov V.I., Matuzenko M.Y., Proskurina O.V. Purity Analysis of Trade Produced C_{60} Fullerene. *Mat. Phys. and Mechanics*, 2012, **18**(3), P. 181–185.

[192] Gerasimov V.I., Trofimov A., Proskurina O. Isomers of Fullerene C_{60}. *Mat. Phys. and Mechanics*, 2014, **20**(1), P. 25–32.

[193] Mendes R.G., Bachmatiuk A., Buchner B., Cuniberti G., Rummeli M.H. Carbon nanostructures as multi-functional drug delivery platforms. *J. Mater. Chem. B*, 2013. **1**(4), P. 401–428.

[194] Mikheev I.V., Bolotnik T.A., Volkov D.S., Korobov M.V., Proskurnin M.A. Approaches to the determination of C_{60} and C_{70} fullerene and their mixtures in aqueous and organic solutions. *Nanosystems: Physics, Chemistry, Mathematics,* 2016, **7**(1), P. 104–110.

[195] Mazur A.S., Karpunin A.E., Proskurina O.V., Gerasimov V.I., Pleshakov I.V., Matveev V.V., Kuz'min Yu.I. Nuclear Magnetic Resonance Spectra of Polyhydroxylated Fullerene $C_{60}(OH)_n$. *Phys. Solid State*, 2018, **60**(7), P. 1468–1470.

[196] Mikheev I.V., Pirogova M.O., Bolotnik T.A., Volkov D.S., Korobov M.V., Proskurnin M.A. Optimization of the solvent exchange process for highyield synthesis of aqueous fullerene dispersions. *Nanosystems: Physics, Chemistry, Mathematics*, 2018, **9**(1), P. 41–45.

[197] Karpunin A.E., Gerasimov V.I., Mazur A.S., Pleshakov I.V., Fofanov Y.A. Proskurina O.V. NMR Investigation of Composite Material, Formed by Fullerenol in Polymer Matrix of Polyvinyl Alcohol. *IEEE International Conference on Electrical Engineering and Photonics (EExPolytech)*, 2018, P. 168–171.

[198] Andrievsky G.V., Klochkov V.K., Bordyuh A., Dovbeshko G.I. Comparative Analysis of Two Aqueous-Colloidal Solution of C60 Fullerene with Help of FT-IR Reflectance and UV-VIS Spectroscopy. *Chem. Phys. Lett.*, 2002, **364**, P. 8–17.

[199] Andrievsky G.V., Bruskov V.I., Tykhomyrov A.A., Gudkov S.V. Peculiarities of the antioxidant and radioprotective effects of hydrated C_{60} fullerene nanostuctures in vitro and in vivo. *Free Radical Biology & Medicine*, 2009, **47**, P. 786–793.

[200] Semenov K.N., Charykov N.A., Postnov V.N., Sharoyko V.V., Murin I.V. Phase equilibria in fullerene-containing systems as a basis for development of manufacture and application processes for nanocarbon materials. *Russ. Chem. Rev.*, 2016, **85**(1), P. 38–59.

[201] Jargalan N., Tropin T.V., Avdeev M.V., Aksenov V.L. Investigation and modeling of evolution of C_{60}/NMP solution UVVis spectra. *Nanosystems: Physics, Chemistry Mathematics*, 2016, **7**(1), P. 99–103.

[202] Mchedlov-Petrossyan N.O., Kamneva N.N., Al-Shuuchi Y.T.M., Marynin A.I., Shekhovtsov S.V., "The peculiar behavior of fullerene C_{60} in mixtures of good' and polar solvents: Colloidal particles in the toluene–methanol mixtures and some other systems", *Colloid Surf. A-Physicochem. Eng. Asp.*, 2016, **509**, P. 631–637.

[203] Charykov N.A., Semenov K.N., Keskinov V.V., Garamova P.V., Tyurin D.P., Semenyuk I.V., Petrenko V.V., Kurilenko A.V., Matuzenko M.Yu., Kulenova N.A., Zolotarev A.A., Letenko D.G. Cryometry data and excess thermodynamic functions in the binary system: water soluble bisadduct of light fullerene C_{70} with lysine. Assymmetrical thermodynamic model of virtual Gibbs energy decomposition – VDAS. *Nanosystems: Physics, Chemistry, Mathematics*, 2017, **8**(3), P. 397–405.

[204] Semenov K.N., Charykov N.A., Iurev G.O., Ivanova N.M., Keskinov V.A., Letenko D.G, Postnov V.N., Sharoyko V.V., Kulenova N.A., Prikhodko I.V., Murin I.V. Physico-chemical properties of the C_{60} - l -lysine water solutions, *J. Mol. Liq.*, 2017, **225**, P. 767–777.

[205] Semenov K.N., Andrusenko E.V., Charykov N.A., Litasova E.V., Panova G.G., Penkova A.V., Murin I.V., Piotrovskiy L.B. Carboxylated Fullerenes: Physico-Chemical Properties and Potential Applications. *Prog. Solid State Chem.*, 2017, **47-48**, P. 19–36.

[206] Tyurin D.P., Kolmogorov F.S., Cherepkova I.A., Charykov N.A., Semenov K.N., Keskinov V.A., Safyannikov N.M., Pukharenko Y.V., Letenko D.G., Segeda T.A., Shaimardanov Z. Antioxidant properties of fullerenol-d. *Nanosystems: Physics, Chemistry, Mathematics*, 2018, **9**(6), P. 798–810.

[207] Safyannikov N.M., Charykov N.A., Garamova P.V., Semenov K.N., Keskinov V.A., Kurilenko A.V., Cherepcova I.A., Tyurin D.P., Klepikov V.V., Matuzenko M.Y., Kulenova N.A., Zolotarev A.A. Cryometry data in the binary systems bisadduct of C_{60} and indispensable aminoacids – lysine, threonine, oxyproline. *Nanosystems: Physics, Chemistry Mathematics*, 2018, **9** (1), P. 46–48.

[208] Dubinina I.A., Kuzmina E.M., Dudnik A.I., Vnukova N.G., Churilov G.N., Samoylova N.A. Study of antioxidant activity of fullerenols by inhibition of adrenaline autoxidation. *Nanosystems: Physics, Chemistry, Mathematics*, 2016, **7**(1), P. 153–157.

[209] Shultz M.D., Duchamp J.C., Wilson J.D., Shu C.Y., Ge J., Zhang J., Gibson H.W., Fillmore H.L. Encapsulation of a radiolabeled cluster inside a fullerene cage, $^{177}Lu_xLu_{(3-x)}N@C_{80}$: an interleukin-13-conjugated radiolabeled metallofullerene platform. *J. Amer. Chem. Soc.*, 2010, **132**(14), P. 4980–4981.

[210] Bolskar R.D. Gadofullerene MRI contrast agents. *Nanomedicine (Lond.)*, 2008, **3**(2), P. 201–213.

[211] Zhen M., Zheng J., Ye L., Li S., Jin C., Li K., Qiu D., Han H., Shu C., Yang Y., Wang C. Maximizing the relaxivity of Gd-complex by synergistic effect of HSA and carboxylfullerene. *ACS Appl. Mater. Interfaces*, 2012, **4**(7), P. 3724–3729.

[212] Lebedev V.T., Kulvelis Yu.V., Runov V.V., Szhogina A.A., Suyasova M.V. Biocompatible water-soluble endometallofullerenes: peculiarities of self-assembly in aqueous solutions and ordering under an applied magnetic field. *Nanosystems: Physics, Chemistry, Mathematics*, 2016, **7**(1), P. 22–29.

[213] Elistratova J., Akhmadeev B., Gubaidullin A., Korenev V., Sokolov M., Nizameev I., Stepanov A., Ismaev I., Kadirov M., Voloshina A., Mustafina A. Nanoscale hydrophilic colloids with high relaxivity and low cytotoxicity based on Gd(III) complexes with Keplerate polyanions. *New J. Chem.*, 2017, **41**, P. 5271–5275.

[214] Kondrin M.V., Brazhkin V.V. Is graphane the most stable carbon monohydride? *Nanosystems: Physics, Chemistry, Mathematics*, 2016, **7**(1), P. 44–50.

[215] Mo K., Jiang T., Sun W., Gu Z. ATP-responsive DNA-graphene hybrid nanoaggregates for anticancer drug delivery. *Biomater.*, 2015, **50**, P. 67–74.

[216] Thabitha P., Shareena D., McShan D., Dasmahapatra A.K., Tchounwou P.B. A Review on Graphene-Based Nanomaterials in Biomedical Applications and Risks in Environment and Health. *Nano-Micro Lett.*, 2018, **10**(53); P. 1–34.

[217] Amirov R.H., Iskhakov M.E., Shavelkina M.B. Synthesis of high purity multilayer graphene using plasma jet. *Nanosystems: Physics, Chemistry, Mathematics*, 2016, **7**(1), P. 60–64.

[218] Ren L., Zhang Y., Cui C., Bi Y., Ge X. Functionalized graphene oxide for anti-VEGF siRNA delivery: preparation, characterization and evaluation in vitro and in vivo. *RSC Adv.*, 2017, **7**, P. 20553–20566.

[219] Seliverstova E.V., Ibrayev N.Kh., Dzhanabekova R.K. Study of graphene oxide solid films prepared by Langmuir–Blodgett technology. *Nanosystems: Physics, Chemistry, Mathematics*, 2016, **7**(1), P. 65–70.

[220] Kondrin M.V., Brazhkin V.V. Is graphane the most stable carbon monohydride? *Nanosystems: Physics, Chemistry, Mathematics*, 2016, **7**(1), P. 44–50.

[221] Iijima S., Ichihashi T. Single-Shell Carbon Nanotubes of 1-nm Diameter. *Nature*, 1993, **363**, P. 603–605.

[222] Tessonnier J.-P., Rosenthal D., Yansen T.W., Hess C., Schuster M.E., Matthey J., Blume R., Girgsdies F., Pfnder N., Timpe O., Su D. Analysis of the structure and chemical properties of some commercial carbon nanostructures. *Carbon*, 2009, **47**, P. 1779–1798.

[223] Trostenson E.T., Ren Z., Chou T.W. Advances in the science and technology of carbon nanotubes and their composites: a review. *Composites Sci. and Technology*, 2001, **61**, P. 1899–1912.

[224] Eletskii A.V. Carbon nanotubes. *Advances in Physical Sciences*, 1997, **167**(9), P. 945–972.

[225] Oncel C., Yurum Y. Carbon Nanotube Syntesis via Catalytic CVD Method: A Review on the Effect of Reaction Parameters. *Fullerenes, Nanotubes and Carbon Nanostructures*, 2006, **14**, P. 17–37.

[226] Resasco D.E., Alvarez W.E., Pompeo F., Balzano L., Herrera J.E., Kitiyanan B., Borgna A. A scalable process for production of single-walled carbon nanotubes (SWNTs) by catalytic disproportionation of CO on a solid catalyst. *J. Nanoparticle Res.*, 2002, **4**, P. 131–136.

[227] Kitiyanan B., Alvarez W.E., Harwell J.H., Resasco D.E. Controlled production of single-wall carbon naotubes by catalutic decomposition of CO on bimetallic Co-Mo catalysts. *Chem. Phys. Lett.*, 2000, **317**, P. 497–503.

[228] Xu, F., Zhao, H., Tse, S.D. Carbon nanotube synthesis on catalytic metal alloys in methane/air counter flow diffusion flames. *Proc. Combust. Inst.*, 2007, **31**, P. 1839–1847.

[229] Nasibulin A.G., Moisala A., Jiang H., Kauppinen E.I. Carbon nanotube synthesis from alcohols by a novel aerosol method. *J. Nanoparticle Res.*, 2006, **8**, P. 465–475.

[230] Sadeghian Z. Large-scale production of multi-walled carbon nanotubes by low-cost spray pyrolysis of hexane. *New Carbon Mater.*, 2009, **24**(1), P. 33–38.
[231] Liu X., Ly J., Han S., Zhang D., Requich A., Thompson E., Zhou C. Syntesis and Electronic Properties of Individual Sihgle-Walled Carbon Nanotube/Pjlypyrrole Composite Nanocables. *Adv. Mater.*, 2005, **17**, P. 2727–2732.
[232] Nasibulin A.G., Moisala A., Brown D.P., Jiang H., Kauppinen E.I. A novel aerosol method for single walled carbon nanotube synthesis. *Chem. Phys. Lett.*, 2005, **402**, P. 227–232.
[233] Nyamori V.O., Nxumalo E.N., Coville N.J. The effect of arylerrocene ring substituents on the synthesis of multi-walled carbon nanotubes. *J. Organomet. Chem.*, 2009, **343**, P. 290–298.
[234] Bronikowski M.J., Willis P.W., Colbert D.T., Smith K.A., Smolley R.E. Gas-phase production of carbon single-walled nanotube fro carbon monoxide via the HiPCO process: A parametric study. *J. Vac. Sci. Technol. A*, 2001, **19**(4), P. 1800–1805.
[235] Ebbesen T.W., Ajayan P.M., Hiura H., Tanigaki K. Purification of nanotubes. *Nature*, 1994, **367**, P. 519.
[236] Hou P.X., Liu C., Cheng H.M. Purification of carbon nanotubes. *Carbon*, 2008, **46**, P. 2003–2025.
[237] Jakubek L.M., Marangoudakis S., Raingo J., Liu X., Lipscombe D., Hurt R.H. The inhibition of neuronal calcium ion channels by trace levels of yttrium released from carbon nanotubes. *Biomater.*, 2009, **30**, P. 6351–6357.
[238] Bianco A., Kostarelos K., Partidos C.D., Prato M. Biomedical applications of functionalized carbon nanotubes. *Chem. Commun. (Cambridge, UK)*, 2005, **5**, P. 571–577.
[239] Singh R., Pantarotto D., McCarthy D. Binding and condensation of plasmid DNA onto functionalized carbon nano-tubes: toward the construction of nanotube-based gene delivery vectors. *J. Am. Chem. Soc.*, 2005, **127**, P. 4388–4396.
[240] Mahmood M., Karmakar A., Fejleh A., Mocan T., Iancu C., Mocan L., Iancu D.T., Xu Y., Dervishi E., Li Z., Biris A.R., Agarwal R., Ali N., Galanzha E.I., Biris A.S., Zharov V.P. Synergistic enhancement of cancer therapy using a combination of carbon nanotubes and antitumor drug. *Nanomed. (London)*, 2009, **4**, P. 883–893.
[241] Liu Z., Fan A.C., Rakhra K., Sherlock S., Goodwin A., Chen X., Yang Q., Felsher D.W., Dai H. Supramolecular stacking of doxorubicin on carbon nanotubes for *in vivo* cancer therapy. *Angew. Chem. Int. Ed. Engl.*, 2009, **41**(48), P. 7668–7672.
[242] Pastorin G., Wu W., Wieckwski S., Briand J.P., Kostarelos K., Prato M., Bianco A. Double functionalization of carbon nanotubes for multimodal drug delivery. *Chem. Commun.*, 2006, **11**, P. 1182–1184.
[243] Kateb B., Yamamoto V., Alizadeh D., Zhang L., Manohara H.M., Bronikowski M.J., Badie B. Multi-walled carbon nanotube (MWCNT) synthesis, preperetion, labeling, and functionalization. *Immunotherapy of Cancer, Methods in Molecular Biology*, 2010, **651**, P. 307–317.
[244] Garcia B.O., Kharissova O.V., Rasika Dias H.V., Servando Aguirre T.F., Salinas Hernandez J. Nanocomposites with antibacterial properties using CNTs with magnetic nanoparticles. *Nanosystems: Physics, Chemistry, Mathematics*, 2016, **7**(1), P. 161–168.
[245] Dastjerdi R., Montazer M. A review on the application of inorganic nanostructured materials in the modification of textiles: Focus on antimicrobial properties. *Coll. Surf. B: Biointerfaces*, 2010, **79**, P. 5–18.
[246] Bocharov G.S., Egin M.S., Eletskii A.V., Kuznetsov V.L. Filling carbon nanotubes with argon. *Nanosystems: Physics, Chemistry, Mathematics*, 2018, **9** (1), P. 85–88.
[247] Jakubek L.M., Marangoudakis S., Raingo J., Liu X., Lipscombe D., Hurt R.H. The inhibition of neuronal calcium ion channels by trace levels of yttrium released from carbon nanotubes. *Biomater.*, 2009, **30**, P. 6351–6357.
[248] Foldvari M., Bagonluri M. Carbon nanotubes as functional excipients for nanomedicines: II. Drug delivery and biocompatibility issues. *Nanomed.*, 2008, **4**(3), P. 183–200.
[249] Cai D., Mataraza J.M., Qin Z.H., Huang Z., Huang J., Chiles T.C., Carnahan D., Kempa K., Ren Z. Highly efficient molecular delivery into mammalian cells using carbon nanotube spearing. *Nat. Methods*, 2005, **2**, P. 449–454.
[250] Turcheniuk K., Mochalin V.N. Biomedical Applications of Nanodiamond (Review). *Nanotechnology*, 2017, **28**, P. 252001–252027.
[251] Rosenholm J.M., Vlasov I.I., Burikov S.A., Dolenko T.A., Shenderova O.A. Nanodiamond Based Composite Structures for Biomedical Imaging and Drug Delivery (Review). *J. Nanosci. Nanotechnol.*, 2015, **15**, P. 959–971.
[252] Kulvelis Y.V., Shvidchenko A.V., Aleksenskii A.E., Yudina E.B., Lebedev V.T., Shestakov M.S., Dideikin A.T., Khozyaeva L.O., Kuklin A.I., Gy T., Rulev M.I., Vul A.Y. Stabilization of detonation nanodiamonds hydrosol in physiological media with poly (vinylpyrrolidone). *Diamond and Related Mater.*, 2018, **87**, P. 78–89.
[253] Girard H., Pager V., Simic V., Arnault J.C. Peptide nucleic acid nanodiamonds: Covalent and stable conjugates for DNA targeting. *RSC Adv.*, 2014, **4**, P. 3566–3572.
[254] Mochalin V.N., Shenderova O., Ho D., Gogotsi Y. The Properties and Applications of Nanodiamonds. *Nature Nanotechnology*, 2011, **7**(1), P. 11–23.
[255] Bokarev A.N., Plastun I.L. Possibility of drug delivery due to hydrogen bonds formation in nanodiamonds and doxorubicin: molecular modeling. *Nanosystems: Physics, Chemistry, Mathematics*, 2018, **9**(3), P. 370–377.
[256] Giammarco J., Mochalin V.N., Haeckel J., Gogotsi Y. The adsorption of tetracycline and vancomycin onto nanodiamond with controlled release. *J. Colloid Interface Sci.*, 2016, **468**, P. 253–261.
[257] Vervald E.N., Laptinskiy K.A., Vlasov I.I., Shenderova O.A., Dolenko T.A. DNA nanodiamond interactions influence on fluorescence of nanodiamonds. *Nanosystems: Physics, Chemistry, Mathematics*, 2018, **9**(1), P. 64–66.
[258] Schimke M., Steinmüller-Nethl D., Kern J., Krüger A., Lepperdinger G. Biofunctionalization of nano-scaled diamond particles for use in bone healing and tissue engineering. *Experimental Gerontology*, 2015, **68**, P. 100.
[259] Chen M., Pierstorff E.D., Li Sh-Y., Lam R., Huang H., Osawa E., Ho D. Nanodiamond-mediated delivery of water-insoluble therapeutics. *ASC Nano*, 2009, **7**(3), P. 2012–2022.
[260] Solomatin A.S., Yakovlev R.Yu., Efremenkova O.V., Sumarukova I.G., Kulakova I.I., Lisichkin G.V. Antibacterial activity of Amikacin immobilized detonation nanodiamond. *Nanosystems: Physics, Chemistry, Mathematics*, 2017, **8**(4), P. 531–534.
[261] Danilenko V.V. On the History of the Discovery of Nanodiamond Synthesis. *Physics of the Solid State*, 2004, **46**(4), P. 595–599.
[262] Vul A.Y., Dideikin A.T., Alexenskii A.E., Baidakova M.V. Detonation nanodiamonds: Synthesis, Properties and Applications. Chapter 2. In: Nanodiamond. Ed. Williams O.A. Published by the Royal Society of Chemistry, Cambridge, 2014, P. 27-48.
[263] Bondar' V.S., Puzyr' A.P. Nanodiamonds for Biological Investigations. *Physics of the Solid State*, 2004. **46**(4), P. 716–719.

[264] Tomchuk O., Volkov D., Bulavin L., Rogachev A., Proskurnin M., Korobov M., Avdeev M. Structural characteristics of aqueous dispersions of detonation nanodiamond and their aggregate fractions as revealed by small-angle neutron scattering *J. Phys. Chem. C*, 2015, **119**(1), P. 794–802.
[265] Kulakova I.I. Surface Chemistry of Nanodiamonds. *Phys. Solid State*, 2004, **46**(4), P. 636–643.
[266] Dideikin A.T., Aleksenskii A.E., Baidakova M.V., Brunkov P.N., Brzhezinskaya M., Davydov V.Y., Levitskii V.S., Kidalov S.V., Kukushkina Y.A., Kirilenko D.A., Shnitov V.V., Shvidchenko A.V., Senkovskiy B.V., Shestakov M.S., Vul A.Y. Rehybridization of carbon on facets of detonation diamond nanocrystals and forming hydrosols of individual particles. *Carbon*, 2017, **122**, P. 737–745.
[267] Greiner N.R., Phillips D.S., Johnson J.D., Volk F. Diamonds in detonation soot. *Nature*, 1988, **333**, P. 440–442.
[268] Xu K., Xue Q. A New Method for Deaggregation of Nanodiamond from Explosive Detonation: Graphitization–Oxidation Method. *Phys. Solid State*, 2004, **46**(4), P. 649–650.
[269] Vervald A.M., Burikov S.A., Vlasov I.I., Shenderova O.A., Dolenko T.A Interactions of nanodiamonds and surfactants in aqueous suspensions. *Nanosystems: Physics, Chemistry, Mathematics*, 2018, **9**(1), P. 49–51.
[270] Zhang Q., Mochalin V.N., Neitzel I., Knoke I.Y., Han J., Klug C.A., Zhou J.G., Lelkes P.I., Gogotsi Y. Fluorescent PLLA-nanodiamond composites for bone tissue engineering. *Biomater.*, 2011, **32**(1), P. 87–94.
[271] Bobrysheva I.V., Kashchenko S.A. *Histology, Cytology, Embryology: Textbook*, Knowledge, Lugansk: 2011, 529 p.
[272] Vasudeva N., Mishra S. *Inderbir Singh's Textbook of Human Histology with Colour Atlas and Practical Guide*. Jaypee Brothers Medical Publishers (P) Ltd, New Delhi, 2014, 439 p.
[273] Bykov V.L. *Special Histology of Human: Textbook*. St. Petersburg: SOTIS, 1999, 301 p.
[274] Krause W.J. *Krause's Essential Human Histology*. Univ. Missouri Columbia, 2005, 315 p. (https://mospace.umsystem.edu/xmlui/bitstream/handle/10355/11238/KrausesEssentialHuman.pdf? sequence=1&isAllowed=y).
[275] Membrino M.A. *Transdermal Delivery of Therapeutic Compounds by Iontophoresis*. University of Florida, 2002, 283 p.
[276] Scheuplein R.J. Mechanism of Percutaneous Absorption: II. Transient Diffusion and the Relative Importance of Various Routes of Skin Penetration. *J. Investigative Dermatol.*, 1967, **48**(1), P. 79–88.
[277] *Methods in Molecular Biology. Permeability Barrier: Methods and Protocols*. Ed. Turksen K., Totowa, NJ: Humana Press, 2011, 439 p.
[278] Zesch A., Schaefer H. Penetrationskinetik von radiomarkiertem Hydrocortison aus verschiedenartigen Salbengrundlagen in die menschliche Haut II. In vivo. *Archives Dermatol. Res.*, 1975, **252**(4), P. 245–256.
[279] Schaefer H., Zesch A., Stüttgen G. *Skin Permeability*. Berlin, Heidelberg: Springer Berlin Heidelberg, 1982, 896 p.
[280] Kuznetsova E.G., Ryzhikova V.A., Salomatina L.A., Sevastianov V.I. Transdermal Drug Delivery and Methods to Enhance It. *Russ. J. Transplant. Artificial Organs*, 2016, **18**(2), P. 152–162.
[281] Asbrill C.S., El-Kattan A.F., Marchiniak B. Enchancement of transdermal drug delivery: chemical and physical approaches. *Crit. Rev. Ther. Drug Carrier Syst.*, 2000, **17**(6), P. 612–658.
[282] Paudel K.S., Milewski M., Swadley C.L. Challenges and opportunities in dermal/transdermal delivery. *Ther. Deliv.*, 2010, **1**(1), P. 109–131.
[283] Hupfeld S., Gravem H. Transdermal therapeutic systems for drug administration. *Tidsskr. Nor. Laegeforen*, 2009, **129**(6), P. 532–533.
[284] Sugino M., Todo H., Sugibayashi K. Skin permeation and transdermal delivery systems of drugs: history to overcome barrier function in the stratum corneum. *Yakugaku Zasshi*, 2009, **129**(12), P. 1453–1458.
[285] Heather Benson A.E. Transdermal Drug Delivery: Penetration Enhancement Techniques. *Current Drug Deliv.*, 2005, **2**, P. 23–33.
[286] Moskvin S.V., Minenkov A.A. The mechanism of transcutaneous drug transfer assisted by laserophoresis. *Klin. Dermatol. Venerol.*, 2010, **5**, P. 78–83.
[287] Polat B.E., Figueroa P.L., Blankschtein D., Langer R. Transport Pathways and Enhancement Mechanisms within Localized and Non-Localized Transport Regions in Skin Treated with Low-Frequency Sonophoresis and Sodium Lauryl Sulfate. *J. Pharm. Sci.*, 2011, **100**(20), P. 512–529.
[288] Naegel A., Heisig M., Wittum G. Detailed Modeling of Skin Penetration An Overview. *Advanced Drug Delivery Reviews*, 2013, **65**(2), P. 191–207.
[289] Guy R.H., Hadgraft J., Maibach H.I. A Pharmacokinetic Model for Percutaneous Absorption. *International Journal of Pharmaceutics*, 1982, **11**(2), P. 119–129.
[290] Frasch H.F., Barbero A.M. Application of Numerical Methods for Diffusion-Based Modeling of Skin Permeation. *Advanced Drug Delivery Reviews*, 2013, **65**(20), P. 208–220.
[291] Mitragotri S., Anissimov Y.G., Bunge A.L., Frasch H.F., Guy R.H., Hadgraft J., Kasting G.B., Lane M.E., Roberts M.S. Mathematical Models of Skin Permeability: An Overview. *International Journal of Pharmaceutics*, 2011, **418**(1), P. 115–129.
[292] Anissimov Y.G., Roberts M.S. Diffusion Modeling of Percutaneous Absorption Kinetics. 1. Effects of Flow Rate, Receptor Sampling Rate, and Viable Epidermal Resistance for a Constant Donor Concentration. *Journal of Pharmaceutical Sciences*, 1999, **88**(11), P. 1201–1209.
[293] Lindstrom T.F., Ayres J.W. Diffusion Model for Drug Release from Suspensions II: Release to a Perfect Sink. *Journal of pharmaceutical sciences*, 1977, **66**(5), P. 662–668.
[294] Todo H., Oshizaka T., Kadhum W., Sugibayashi K. Mathematical Model to Predict Skin Concentration after Topical Application of Drugs. *Pharmaceutics*, 2013, **5**(4), P. 634–651.
[295] Guy R.H., Hadgraft J., Maibach H.I. A Pharmacokinetic Model for Percutaneous Absorption. *International Journal of Pharmaceutics*, 1982, **11**(2), P. 119–129.
[296] Guy R.H., Hadgraft J. Transdermal Drug Delivery: A Simplified Pharmacokinetic Approach. *Int. J. Pharm.*, 1985, **24**(2–3), P. 267–274.
[297] Riegelman S. Pharmacokinetics; Pharmacokinetic Factors Affecting Epidermal Penetration and Percutaneous Absorption. *Clinical Pharmacology & Therapeutics*, 1974, **16**(5, part 2), P. 873–883.
[298] Tojo K. Mathematical Modeling of Transdermal Drug Delivery. *Journal of Chemical Engineering of Japan*, 1987, **20**(3), P. 300–308.
[299] Vieth W.R., Howell J.M., Hsieh J.H. Dual Sorption Theory. *Journal of Membrane Science*, 1976, **1**, P. 177–220.
[300] Chandrasekaran S., Michaels A., Campbell P., Shaw J. Scopolamine Permation through Human Skin in Vitro. *AIChE Journal*, 1976, **22**(5), P. 828–832.
[301] Chandrasekaran S.K., Bayne W., Shaw J.E. Pharmacokinetics of Drug Permeation through Human Skin. *Journal of pharmaceutical sciences*, 1978, **67**(10), P. 1370–1374.

[302] Shen J., Kromidas L., Schultz T., Bhatia S. An in silico skin absorption model for fragrance materials. *Food and Chemical Toxicology*, 2014, **74**, P. 164–176.
[303] Flynn G. Physiochemical Determinants of Skin Absorption. In *Principles of route-to-route extrapolation for risk assessment* / Ed. Gerrity T.R., Henry C.J. New York: Elsevier, 1990, P. 93–127.
[304] Barratt M. Quantitative Structure-Activity Relationships for Skin Permeability. *Toxicology in Vitro*, 1995, **9**(1), P. 27–37.
[305] Godin B., Touitou E. Transdermal Skin Delivery: Predictions for Humans from in Vivo, Ex Vivo and Animal Models. *Advanced Drug Delivery Reviews*, 2007, **59**(11), P. 1152–1161.
[306] Potts R.O., Guy R.H. Predicting Skin Permeability. *Pharmaceutical Research*, 1992, **9**(5), P. 663–669.
[307] Geinoz S., Guy R.H., Testa B., Carrupt P.-A. Quantitative Structure-Permeation Relationships (QSPeRs) to Predict Skin Permeation: A Critical Evaluation. *Pharmaceutical Research*, 2004, **21**(1), P. 83–92.
[308] Enbäck J., Laakkonen P. Tumour-homing peptides: tools for targeting, imaging and destruction. *Biochemical Society Transactions*, 2007, **35**(4), P. 780–783.
[309] Un F., Zhou B., Yen Y. The Utility of Tumor-specifically Internalizing Peptides for Targeted siRNA Delivery into Human Solid Tumors. *Anticancer Research*, 2012, **32**, P. 4685–4690.
[310] Rihova B. Targeting of Drugs to Cell Surface Receptors. *Critical Reviews in Biotechnology*, 1997, **17**(2), P. 149–169.
[311] Ivonin A.G., Pimenov E.V., Oborin V.A., Devrishov D.A., Kopylov S.N. Directed Transport of Drugs: Current State and Prospects. *Proceedings of the Komi Science Centre of the Ural Division of the Russian Academy of Sciences*, 2012, **1**(9), P. 46–55.
[312] Guillemard V., Uri Saragovi N. Prodrug chemotherapeutics bypass p-glycoprotein resistance and kill tumors in vivo with high efficacy and target-dependent selectivity. *Oncogene*, 2004, **23**(20), P. 3613–3621.
[313] Baselga J. A review of EGFR targeted therapy. *Clin. Adv. Hemato.l Oncol.*, 2003, **1**(4), P. 218–219.
[314] Sharman W.M., van Lier J.E., Allen C.M. Targeted photodynamic therapy via receptor mediated delivery systems. *Adv. Drug Deliv. Rev.*, 2004, **56**(1), P. 53–76.
[315] Manoharan M. Oligonucleotide conjugates as potential antisense drugs with improved uptake, biodistribution, targeted delivery, and mechanism of action. *Antisense Nucieic Acid Drug Dev.*, 2002, **12**(2), P. 103–128.
[316] Stern M., Herrmann R. Overview of monoclonal antibodies in cancer therapy: present and promise. *Crit. Rev. Oncol. Hematol.*, 2005, **54**(1), P. 11–29.
[317] Casi G., Neri D. Antibody-drug conjugates: basic concepts, examples and future perspectives. *J. Cont. Release*, 2012, **161**(2), P. 422–428.
[318] Wei, C., Su, D., Wang, J., Jian W., Zhang D. LC–MS Challenges in Characterizing and Quantifying Monoclonal Antibodies (mAb) and Antibody-Drug Conjugates (ADC) in Biological Samples. *Curr. Pharmacol. Rep.*, 2018, **4**(1), P. 45–63.
[319] Bareford L.M., Swaan P.W. Endocytic mechanisms for targeted drug delivery. *Adv. Drug. Deliv. Rev.*, 2007, **59**(8), P. 748–758.
[320] Marsh M., McMahon H.T. The structural era of endocytosis. *Science*, 1999, **285**(5425), P. 215–220.
[321] Mousavi S.A., Malerod L., Berg T., Kjeken R. Clathrin-dependent endocytosis. *Biochem. J.*, 2004, 377(1), P. 1–16.
[322] Rodemer C., Haucke V. Clathrin/AP-2-dependent endocytosis: a novel playground for the pharmacological toolbox? *Handb. Exp. Pharmacol.*, 2008, **186**, P. 105–122.
[323] Krippendorff B.F., Kuester K., Kloft C., Huisinga W. Nonlinear pharmacokinetics of therapeutic proteins resulting from receptor mediated endocytosis. *J. Pharmacokinet. Pharmacodyn.*, 2009, **36**(3), P. 239–260.
[324] Khalil I.A., Kogure K., Akita H., Harashima H. Uptake pathways and subsequent intracellular trafficking in nonviral gene delivery. *Pharmacol. Rev.*, 2006, **58**(1), P. 32–45.
[325] Rawat A., Vaidya B., Khatri K., Goyal A.K., Gupta P.N., Mahor S., Paliwal R., Rai S., Vyas S.P. Targeted intracellular delivery of therapeutics: an overview. *Die Pharmazie*, 2007, **62**(9), P. 643–658.
[326] Bildstein L., Dubernet C., Couvreur P. Prodrug-based intracellular delivery of anticancer agents. *Adv. Drug. Deliv. Rev.*, 2011, **63**(1-2), P. 3–23.
[327] Yu S., Li A., Liu Q., Li T., Yuan X., Han X., Wu K. Chimeric antigen receptor T cells: a novel therapy for solid tumors. *J. Hematol. Oncol.*, 2017, **10**(1), P. 1–13.
[328] Rosenkranz A.A,, Ulasov A.V., Slastnikova T.A., Khramtsov Y.V., Sobolev A.S. Use of Intracellular Transport Processes for Targeted Drug Delivery into a Specified Cellular Compartment. *Biochem. (Moscow)*, 2014, **79**(9), P. 928–946.
[329] Pauling L. *The Nature of the Chemical Bond*, 3-d edition. Itaca, New York, Cornell University Press, London, Oxford University Press,1960, 643 p.
[330] Yamase T. Polyoxometalates for Molecular Devices: Antitumor Activity and Luminescence. *Molecular Eng.*, 1993, **3**(1–3), P. 241–262.
[331] Yamase T., Fujita H., Fukushima K. Medical Chemistry of Polyoxometalates. Part 1. Potent Antitumor Activity of Polyoxomolybdates on Animal Transplantable Tumors and Human Cancer Xenograft. *Inorg. Chim. Acta*, 1988, **151**(1), P. 15–18.
[332] Yang H.-K., Cheng Y.-X., Su M.-M., Xiao Y., Hu M.-B., Wang W., Wang Q. Polyoxometalate–biomolecule Conjugates: A New Approach to Create Hybrid Drugs for Cancer Therapeutics. *Bioorganic & Med. Chem. Lett.*, 2013, **23**(5), P. 1462–1466.
[333] Bijelic A., Aureliano M., Rompel A. Polyoxometalates as Potential Next-Generation Metallodrugs in the Combat Against Cancer. *Angew. Chem. Int. Ed.*, 2019, **58**, P. 2980–2999.
[334] Datta L.P., Mukherjee R., Subharanjan Biswas S., Das T.K. Peptide-Based Polymer-Polyoxometalate Supramolecular Structure with a Differed Antimicrobial Mechanism. *Langmuir*, 2017, **33**, P. 14195–14208.
[335] Müller A., Krickemeyer E., Bögge H., Schmidtmann M., Peters F. Organizational Forms of Matter: An Inorganic Super Fullerene and Keplerate Based on Molybdenum Oxide. *Angew. Chem. Int. Ed.*, 1998, **37**(24), P. 3359–3363.
[336] Müller A., Gouzerh P. From Linking of Metal-Oxide Building Blocks in a Dynamic Library to Giant Clusters with Unique Properties and towards Adaptive Chemistry. *Chem. Soc. Rev.*, 2012, **41**(22), P. 7431–7463.
[337] Awada M., Floquet S., Marrot J., Haouas M., Morcillo S.P., Bour Ch., Gandon V., Coeffard V., Greck Ch., Cadot E. Synthesis and Characterizations of Keplerate Nanocapsules Incorporating L- and D-Tartrate Ligands. *J. Clust. Sci.*, 2017, **28**(2), P. 799–812.
[338] Ostroushko A.A., Adamova L.V., Eremina E.V., Grzhegorzhevskii K.V. Interaction between nanocluster polyoxometallates and low-molecular-weight organic compounds. *Russ. J. Phys. Chem. A*, 2015, **89**(8), P. 1439–1444.
[339] Tonkushina M.O., Gagarin I.D., Grzhegorzhevskii K.V., Ostroushko A.A. Electrophoretic Transfer of Nanocluster Polyoxometalate $Mo_{72}Fe_{30}$ Associates through the Skin Membrane. *Bull. Ural Med. Acad. Sci.*, 2014, **3**(49), P. 59–61.

[340] Ostroushko A.A., Grzhegorzhevskii K.V. Electric Conductivity of Nanocluster Polyoxomolybdates in the Solid State and Solutions. *Russ. J. Phys. Chem. A*, 2014, **88**(6), P. 1008–1011.

[341] Müller A., Shah S. Q. N., Bögge H., Schmidtmann M., Sarkar S., Kögerler P., Hauptfleisch B., Trautwein A.X, Schönemann V. Archimedean Synthesis and Magic Numbers:"Sizing" Giant Molybdenum-Oxide-Based Molecular Spheres of the Keplerate Type. *Angew. Chem. Int. Ed.*, 1999, **38**(21), P. 3238–3241.

[342] Ostroushko A.A., Tonkushina M.O., Korotaev V.Yu., Prokof'eva A.V., Kutyashev I.B., Vazhenin V.A., Danilova I.G., Men'shikov S.Yu. Stability of the $Mo_{72}Fe_{30}$ Polyoxometalate Buckyball in Solution. *Russ. J. Inorg. Chem.*, 2012. **57**(9), P. 1210–1213.

[343] Ostroushko A.A., Tonkushina M.O. Destruction of Molybdenum Nanocluster Polyoxometallates in Aqueous Solutions. *Russ. J. Phys. Chem. A*, 2015, **89**(3), P. 443–446.

[344] Ostroushko A.A., Danilova I.G., Gette I.F., Medvedeva S.Yu., Tonkushina M.O., Prokofieva A.V., Morozova M.V. Study of Safety of Molybdenum and Iron-Molybdenum Nanocluster Polyoxometalates Intended for Targeted Delivery of Drugs. *J. Biomat. Nanobiotechnol.*, 2011, **2**(5), P. 557–560.

[345] Ostroushko A.A., Gette I.F., Medvedeva S.Y., Danilova I.G., Mukhlynina E.A., Tonkushina M.O., Morozova M.V. Study of Acute and Subacute Action of Iron-Molybdenum Nanocluster Polyoxometalates. *Nanotechnologies in Russia*, 2013, **8**(9–10), P. 672–677.

[346] Gette I.F., Medvedeva S.Yu., Ostroushko A.A. Condition of the Immune System Organs and Blood Leucocytes in Rats after the Exposition of Iron-Molybdenum Polyoxometalates. *Russian J. of Immunol.*, 2017, **11**(2),P. 280–282

[347] Danilova I.G., Gette I.F., Medvedeva S.Y., Mukhlynina E.A., Tonkushina M.O., Ostroushko A.A. Changing the Content of Histone Proteins and Heat-Shock Proteins in the Blood and Liver of Rats after the Single and Repeated Administration of Nanocluster Iron-Molybdenum Polyoxometalates. *Nanotechnologies in Russia*, 2015, **10**(9–10), P. 820–826.

[348] Liu T., Imber B., Diemann E., Liu G., Cokleski K., Li H., Chen Z., Müller A. Deprotonations and Charges of Well-Defined $Mo_{72}Fe_{30}$ Nanoacids Simply Stepwise Tuned by pH Allow Control/Variation of Related Self-Assembly Processes. *J. Am. Chem. Soc.*, 2006, **128**(49), P. 15914–15920.

[349] Ostroushko A.A., Gette I.F., Danilova I.G., Mukhlynina E.A., Tonkushina M.O., Grzhegorzhevskii K.V. Studies on the Possibility of Introducing Iron–Molybdenum Buckyballs into an Organism by Electrophoresis. *Nanotechnologies in Russia*, 2014, **9**(9–10), P. 586–591.

[350] Ostroushko A.A., Danilova I.G., Gette I.F., Tonkushina M.O., Behavior of Associates of Keplerate-Type Porous Spherical $Mo_{72}Fe_{30}$ Clusters with Metal Cations in Electric Field-Driven Ion Transport. *Russ. J. Inorg. Chem.*, 2015, **60**(4), P. 500–504.

[351] Ostroushko A.A., Grzhegorzhevskii K.V., Bystrai G.P., Okhotnikov S.A. Modeling the Processes of Electrophoretic Transfer for Spherical Nanoclusters of Iron–Molybdenum Polyoxometalates. *Russ. J. Phys. Chem. A*, 2015, **89**(9), P. 1638–1641.

[352] Michelis F.V., Delitheos A., Tiligada E. Molybdate modulates mitogen and cyclosporin responses of human peripheral blood lymphocytes. *J. Trace Elements in Med. and Biol.*, 2011, **25**, P. 138–142.

[353] Müller A., Sarkar S., Shah S.Q.N., Bögge H., Schmidtmann M., Sarkar S., Kögerler P., Hauptfleisch B., Trautwein V.X., Schünemann V. Archimedean Synthesis and Magic Numbers: "Sizing" Giant Molybdenum-Oxide-Based Molecular Spheres of the Keplerate Type. *Angew. Chem. Int. Ed. Engl.*, 1999, **38**(21), P. 3238–3241.

[354] Ostroushko A.A., Tonkushina M.O., Martynova N.A. Mass and charge transfer in systems containing nanocluster molybdenum polyoxometallates with a fullerene structure. *Russ. J. Phys. Chem. A*, 2010, **84**(6), P. 1022–1027.

[355] Gagarin I.D., Kulesh N.A., Tonkushina M.O., Vlasov D.A., Ostroushko A.A. Physico-chemical aspects of electrotransport of keplerate-type nanocluster polyoxoanions in native membranes. *Physical and chemical aspects of the study of clusters, nanostructures and nanomaterials*, 2017, **9**, P. 147–152.

[356] Bystrai G.P. *Thermodynamics of irreversible processes in open systems. (Termodinamika neobratimykh processov w otkrytykh sistemakh)*, Moscow - Izhevsk: Research Center of Regular and Random Dynamics, 2011. 264 pp. (in Russian)

[357] Prigogine I. *Introduction to Thermodynamics of Irreversible Processes*, 3-rd Ed., Interscience Publishers, a division of John Wiley & Sons New York, London, Sydney, 1967, 146 p.

[358] Kahaner D., Moler C., Nash S. *Numerical Methods and Software*, Prentice Hall, 1989, 495 p.

[359] Kamont Z., Czernous W. Implicit Difference Methods for Hamilton-Jacobi Functional Differential Equations. *Numerical Anal. Appl.*, 2009, **2**(1), P. 46–57.

[360] Ardelyan I.V. On the use of iterative nethods when realizing implicit difference schemes of two-dimensional magnetohydrodynamics. *USSR Comp. Mathem. Mathem. Phys.*, 1983, **23**(6), P. 84–90.

[361] Czernous W. Implicit Difference Methods for Hamilton-Jacobi Functional Differential Equations. *Numerical Anal. Appl.*, 2009, **2**(1), P. 46–57.

[362] Gu X.M., Huang T.Z., Ji C.C., Carpentieri B., Alikhanov A.A. Fast Iterative Method with a Second-Order Implicit Difference Scheme for Time-Space Fractional Convection–Diffusion Equation. *J. Sci. Comp.*, 2017, **72**(3), P. 957–985.

[363] Shikhova S.V. The Genotoxic Effect of Aminopterin and Methotrexate on Fertility of Several Lines Wild Type of Drosophila Melanogaster. *Proceedings of Voronezh State University. Series Chem., Biol., Pharm.*, 2017, **4**, P. 93–98.

[364] Ostroushko A.A., Gagarin I.D., Grzhegorzhevskii K., Gette I.F., Vlasov D.A., Ermoshin F.A., Antosyuk O.N., Shikhova S.V., Danilova I.G. New Aspects of Studying of Physico-chemical Propertis of Nanocluster Polyoxomolybdates as Perspective Materials for Biomedicine. Conferences Cluster 2018. X International Conference "Kinetics and mechanism of crystallization". July 1-6, 2018, Suzdal, Russia. P. 29–30.

[365] Shikhova S.V., Grzhegorzhevskii K.V., Gagarin I.D. Assessment of address delivery efficiency of aminopterin by means of iron-molybdenum nanocluster polyoxometalat with use of the biotest. Transactions of the XVth All-Russian scientific and practical Conference with international participation "Biodiagnostics of a Condition of Natural and Natural-Technogenic Systems". Kirov. 4-6 Dec. 2017. Kirov: Vyatka State University, 2017, P. 198–202.

[366] Ostroushko A.A., Safronov A.P., Tonkushina M.O., Korotaev V.Yu., Barkov A.Yu. Interaction between Mo_{132} Nanocluster Polyoxometalate and Solvents. *Russ. J. Phys. Chem. A*, 2014, **88**(12), P. 2179–2182.

[367] Ostroushko A.A., Gagarin I.D., Tonkushina M.O., Grzhegorzhevskii K.V., Danilova I.G., Gette I.F., Kim G.A. Iontophoretic Transport of Associates Based on Porous Keplerate-Type Cluster Polyoxometalate $Mo_{72}Fe_{30}$ and Containing Biologically Active Substances. *Russ. J. Phys. Chem. A*, 2017, **91**(9), P. 1811–1815.

[368] Timin A.S., Solomonov A.V., Musabirov I.I. Sergeev S.N., Ivanov S.P., Rumyantsev E.V., Goncharenko A. Immobilization of bovine serum albumin onto porous poly (vinylpyrrolidone)-modified silicas. *Ind. Eng. Chem. Res.*, 2014, **53**(35), P. 13699–13710.

[369] Kadajji V.G., Betageri G.V. Water Soluble Polymers for Pharmaceutical Applications. *Polymers*, 2011, **3**, P. 1972–2009.

[370] Ostroushko A.A., Safronov A.P., Tonkushina M.O. Thermochemical Study of Interaction between Nanocluster Polyoxomolybdates and Polymers in Film Compositions. *Russ. J. Phys. Chem. A*, 2014, **88**(2), P. 295–300.

[371] Bijelic A., Rompel A. The use of polyoxometalates in protein crystallography – An attempt to widen a well-known bottleneck. *Coord. Chem. Rev.*, 2015, **299**, P. 22–38.

[372] Gagarin I., Tonkushina M., Ostroushko A. Stabilization of keplerate-type spheric porous nanocluster polyoxometalate $Mo_{72}Fe_{30}$. 2018 Ural Symposium on Biomedical Engineering, Radioelectronics and Information Technology (USBEREIT), 2018, P. 41–44.

[373] Cedervall T., Lynch I., Lindman S., Berggard T., Thulin E., Nilsson H., Dawson K.A., Linse S. Understanding the nanoparticle–protein corona using methods to quantify exchange rates and affinities of proteins for nanoparticles. *Proc. Natl Acad. Sci. USA*, 2007, **104**, P. 2050–2055.

[374] Lundqvist M., Stigler J., Elia G., Lynch I., Cedervall T., Dawson K.A. Nanoparticle size and surface properties determine the protein corona with possible implications for biological impacts *Proc. Natl Acad. Sci. USA*, 2008, **105**, P. 14265–14270.

[375] Casals E., Pfaller T., Duschl A., Oostingh G.J., Puntes V. Quantitative study of protein coronas on gold nanoparticles with different surface modifications. *ACS Nano*, 2010, **4**, P. 3623–3632.

[376] Docter D., Westmeier D., Markiewicz M., Stolte S., Knauer S.K., Stauber R.H. The nanoparticle biomolecule corona: lessons learned – challenge accepted? *Chem. Soc. Rev.*, 2015, **44** P. 6094–6121.

[377] Walkey C.D., Olsen J.B., Song F., Liu R., Guo H., Olsen D.W.,Cohen Y., Emili A., Chan W.C. Protein corona fingerprinting predicts the cellular interaction of gold and silver nanoparticles. *ACS Nano*, 2014, **8** P. 2439–2455.